AD-A035 376 TENNESSEE UNIV KNOXVILLE ULTRASONICS LAB F/G 20/1
AN ULTRASONIC INVESTIGATION OF THE NONLINEARITY OF FUSED SILICA--ETC(U)
JAN 77 J H CANTRELL N00014-71-A-0121-0001
UNCLASSIFIED TR-14 NL

1 OF 2
AD-A
035 376

AD-A035 376

AN ULTRASONIC INVESTIGATION OF THE NONLINEARITY OF FUSED SILICA FOR DIFFERENT HYDROXYL ION CONTENTS AND HOMOGENEITIES BETWEEN 300 DEG. AND 3 DEG. K

TENNESSEE UNIVERSITY, KNOXVILLE

JANUARY 1977

OFFICE OF NAVAL RESEARCH
CONTRACT NO. N00014-71-A-0121-0001
PROJECT NO. 384-306

TECHNICAL REPORT NO. 14

AN ULTRASONIC INVESTIGATION OF THE NONLINEARITY OF FUSED SILICA FOR DIFFERENT HYDROXYL ION CONTENTS AND HOMOGENEITIES BETWEEN 300° AND 3° K

JOHN H. CANTRELL, JR.

M.A. BREAZEALE
PRINCIPAL INVESTIGATOR
ULTRASONICS LABORATORY
DEPARTMENT OF PHYSICS

THE UNIVERSITY OF TENNESSEE
Knoxville, Tennessee

January 1977

AN ULTRASONIC INVESTIGATION OF THE NONLINEARITY OF FUSED SILICA FOR DIFFERENT HYDROXYL ION CONTENTS AND HOMOGENEITIES BETWEEN 300° AND 3° K

by

John H. Cantrell, Jr.

OFFICE OF NAVAL RESEARCH

CONTRACT NO. N00014-71-A-0121-0001
PROJECT NO. 384-306

TECHNICAL REPORT NO. 14

Ultrasonics Laboratory
Department of Physics
The University of Tennessee
Knoxville, Tennessee
37916

January 1977

1a

A

PREFACE

The third-order elastic constants C_{111} of four types of fused silica were measured as a function of temperature between room temperature and 3° K. The room temperature values were determined absolutely by measuring the harmonic distortion of an initially sinusoidal ultrasonic wave propagating through the sample. Relative values were measured at lower temperatures. The results indicate that a relatively large OH content in fused silica gives rise to a relatively large value of C_{111} and that C_{111} is a weak function of temperature regardless of OH content.

The relationship between the experimentally defined ultrasonic nonlinearity parameter $\beta = -\frac{3C_{11} + C_{111}}{3C_{11}}$ and the Grüneisen parameter γ also has been determined.

This report is an adaptation of the dissertation of John H. Cantrell, Jr. submitted to the Department of Physics at The University of Tennessee in partial fulfillment of the requirements of the degree of Doctor of Philosophy.

The author wishes to express his sincere appreciation to Professor M. A. Breazeale for his advice and guidance in this investigation, and for his patience and understanding. He extends a special thank you to Professor A. Zarembowitch of the Université Pierre et Marie Curie, Paris, France, for sending data on the temperature dependence of the second-order elastic constants. He is indebted to Dr. W. T. Yost for his help during various stages of this research and to Dr. Laszlo Adler for his enlightening discussions.

Unclassified

Security Classification

DOCUMENT CONTROL DATA - R&D

(Security classification of title, body of abstract and indexing annotation must be entered when the overall report is classified)

1. ORIGINATING ACTIVITY (Corporate author)
Ultrasonics Laboratory, Department of Physics
The University of Tennessee
Knoxville, Tennessee 37916

2a. REPORT SECURITY CLASSIFICATION
Unclassified

2b. GROUP

3. REPORT TITLE
An Ultrasonic Investigation of the Nonlinearity of Fused Silica for Different Hydroxyl Ion Contents and Homogeneities between 300° and 3° K

4. DESCRIPTIVE NOTES (Type of report and inclusive dates)
Technical Report No. 14

5. AUTHOR(S) (Last name, first name, initial)
John H. Cantrell, Jr.

6. REPORT DATE	7a. TOTAL NO. OF PAGES	7b. NO. OF REFS
January 1977	104	76

8a. CONTRACT OR GRANT NO.	9a. ORIGINATOR'S REPORT NUMBER(S)
N00014-71-A-0121-0001	Technical Report No. 14
b. PROJECT NO. 384-306	
c.	9b. OTHER REPORT NO(S) (Any other numbers that may be assigned this report)
d.	

10. AVAILABILITY/LIMITATION NOTICES
Distribution of this document is unlimited

11. SUPPLEMENTARY NOTES	12. SPONSORING MILITARY ACTIVITY
	Office of Naval Research, Code 468 Department of the Navy Arlington, Virginia 22217

13. ABSTRACT

The third-order elastic constants C_{111} of four types of fused silica were measured as a function of temperature between room temperature and 3° K. The room temperature values were determined absolutely by measuring the harmonic distortion of an initially sinusoidal ultrasonic wave propagating through the sample. Relative values were measured at lower temperatures. The results indicate that a relatively large OH content in fused silica gives rise to a relatively large value of C_{111} and that C_{111} is a weak function of temperature regardless of OH content.

The relationship between the experimentally defined ultrasonic nonlinearity parameter

$$\beta = -\frac{3C_{11} + C_{111}}{3C_{11}}$$

and the Grüneisen parameter γ also has been determined.

DD FORM 1 JAN 64 1473

Unclassified

Security Classification

The author acknowledges the assistance of Mr. M. A. Torbett with most of the helium transfers and that of Messrs. D. K. Lewis and E. E. Bridges, Jr. for the remainder of them. He thanks Dr. J. A. Bains, Jr. for his discussions on the electronics.

The author is grateful to the National Institutes of Health, the United States Office of Naval Research, and The University of Tennessee Department of Physics for providing financial assistance during his graduate studies.

TABLE OF CONTENTS

CHAPTER I

INTRODUCTION

A number of the physical properties of solids result from the fact that solids are inherently nonlinear. Among the properties are thermal expansion, attenuation of high frequency sound waves, heat conduction, pressure variations of second-order elastic constants, and waveform distortion of sound waves passing through a solid. These nonlinear effects arise because of anharmonicity of the interatomic potential (the deviation from a potential that is quadratic in the interatomic displacement from equilibrium).

In the present experiments anharmonicity is investigated from the distortion of ultrasonic waves passing through a solid, and the results are related to the Grüneisen parameter which is a thermodynamic measure of nonlinearity in solids.

Previously the investigation of anharmonicity in solids has been pursued from the more purely thermodynamic investigations. Thermal expansion has been among the most measured of the thermodynamic properties, and data for many materials have been available for many years. For example, Fizeau (1863) was among the earliest investigators to measure thermal expansion.

Grüneisen (1926) developed the relationship between the thermal expansion coefficient and a parameter which was assumed to be temperature independent (the Grüneisen parameter γ). Barron (1955) and Sheard (1958)

were among the first to make calculations relating the Grüneisen parameter to elastic data. They limited their calculations to the cases of high and low temperatures. Collins (1963), Schuele and Smith (1964), Brugger and Fritz (1967), and Gerlich (1975) made more extensive calculations to include the temperature dependence of the Grüneisen parameter from elastic data, using the quasiharmonic Debye model of solids. Thus, the Grüneisen constant is a convenient link between thermal expansion data and elastic data.

The agreement of the calculated dependence of the Grüneisen parameter as a function of temperature with values measured from thermal expansion has been limited, because of the lack of availability of elastic data (particularly third-order elastic constants) as a function of temperature. For many materials such as Cu, Ag, Au, Al, and Na qualitative agreement exists but some materials exhibit an anomalous behavior of the thermal expansion coefficient as a function of temperature. One such material is fused silica. Fused silica has a positive thermal expansion coefficient until it reaches a temperature between .3 and .4 of its Debye temperature. In that range the thermal expansion coefficient becomes negative and continues to grow more negative as the temperature is lowered (White, 1964). Several investigations (Clark and Strakna, 1962; White, 1964; Klein and Mountain, 1962; McCammon and White, 1963) indicate that at least part of the explanation for this behavior of fused silica may be due to the dominance of transverse acoustic modes at these temperatures; however, this hypothesis can be tested only as information on the behavior of third-order elastic (TOE) constants as functions of temperature is collected. Since the

third-order elastic constants determine how a large amplitude ultrasonic wave distorts as it propagates through the solid, TOE constants can be calculated from ultrasonic wave distortion.

The distortion of an ultrasonic wave as it passes through a solid may be studied by use of either classical continuum mechanics or quantum mechanics. Classically, this phenomenon may be described by a nonlinear wave equation whose solution predicts the growth of higher harmonics as the wave propagates through the solid. Quantum mechanically, this is equivalent to two phonons of one frequency interacting to produce one phonon at the second harmonic of that frequency. Both descriptions depend upon the introduction of terms of order higher than quadratic in the strain potential energy function of the solid. The coefficients (elastic constants) of the power series expansion of the strain potential energy function are related to the coefficient (force constants) of the power series expansion of the interatomic potential function. For example, Coldwell-Horsfall (1963) gave a relation between force constants between molecules in a cubic crystal and the elastic constants of the solid, and Ghate (1965) used the Born model of ionic solids to compute the third-order elastic constants of alkali halides.

Several experimental techniques have been used to determine the nonlinear behavior of solids. Hughes and Kelley (1953) were first to obtain the complete set of third-order elastic (TOE) constants for isotropic materials by measuring the variation of ultrasonic wave velocity with hydrostatic pressure and with uniaxial stress in polystyrene, iron, and pyrex glass. Skove and Powell (1967) pointed out

that these TOE constants are neither truly adiabatic nor isothermal since they result from the superposition of an adiabatic wave on an isothermal stress. Bateman, Mason, and McSkimin (1961) had obtained the first complete set of such "mixed" TOE constants for a cubic crystal (germanium) using this method.

Classical calculations of the interaction of two intersecting ultrasonic beams were made by Jones and Kobett (1963) to determine various combinations of TOE constants. The quantum mechanical treatment of the same experimental situation was made by Taylor and Rollins (1964). Experimental results have been reported by Rollins (1963), Rollins, Taylor, and Todd (1964), and Dunham and Huntington (1970).

Barker and Hollenbach (1970) and Graham (1972) measured the strain resulting in a sample struck by a projectile to calculate the third- and higher-order elastic constants of solids. Melngailis, Maradudin, and Seeger (1963) measured TOE constants from the asymmetry of the diffraction pattern produced by light propagating through a transparent solid in which a finite amplitude ultrasonic wave is propagating.

The method used in the present experiments involves the measurement of waveform distortion of an ultrasonic wave as it propagates through the solid. A pure sinusoidal wave is introduced into the sample and the nonlinearity of the medium causes the generation of harmonics as the wave propagates. This effect was first reported by Gedroits and Krasilnikov (1963) and independently by Breazeale and Thompson (1963). Breazeale and Ford (1965) solved the nonlinear equations of motion describing this effect for isotropic solids and cubic crystals. Gauster and Breazeale (1965) developed a capacitive receiver capable of

measurement of the absolute amplitude of the fundamental and harmonics of the ultrasonic waveform after propagation through the solid and calculated the TOE constants of Copper. Yost and Breazeale (1973) used this receiver to measure fused silica and combined the results with those of Dunham and Huntington (1970) to obtain the first complete set of truly adiabatic TOE constants.

Mackey and Arnold (1969) and Meeks and Arnold (1970) used this method to measure combinations of TOE constants from room temperature to 100 °K. Peters, Breazeale, and Paré (1968) developed a pneumatically controlled variable gap capacitive receiver capable of making accurate measurements at lower temperatures. Peters, Breazeale, and Paré (1970) measured combinations of TOE constants of copper to liquid nitrogen temperatures, and Yost and Breazeale (1974) made similar measurements on germanium. Bains and Breazeale (1976) extended the capability of this technique to liquid helium temperatures for measurements on germanium.

In the experiments described in this dissertation the apparatus of Bains (1974) was used to measure harmonic distortion of a 30 MHz ultrasonic wave in four types of fused silica. The TOE constants are measured between room temperature and 3 °K, and their behavior as a function of temperature is related to that of the Grüneisen parameter.

In Chapter II the theory of ultrasonic nonlinearity in solids is discussed, and the relationship between measured quantities and TOE constants is derived. The relationship between the TOE constants and the Grüneisen parameter is examined in Chapter III. Apparatus,

procedure, and samples are discussed in Chapter IV. Finally, Chapter V presents results of measurements on fused silica, and discussion of the implications of these measurements.

CHAPTER II

THEORY OF ULTRASONIC NONLINEARITY IN SOLIDS

The theory of a finite amplitude ultrasonic wave propagating through a solid medium may be approached either from a quantum mechanical point of view or from classical continuum mechanics. Quantum mechanically we may consider three-phonon interaction processes to calculate transition probabilities using appropriate interaction Hamiltonians. These transition probabilities yield the corresponding classical results when integration is performed over the appropriate interaction volume (Bajak, 1976).

The interaction volume is typically more than twenty orders of magnitude greater than primitive cell (intermolecular) volumes and for this reason the approach of continuum mechanics is justified. Hence, the distortion of an ultrasonic wave as it propagates through the solid can be described by a solution to the nonlinear wave equation obtained from Lagrange's equation for a continuum. The nonlinear terms in the wave equation enter in two ways. First, the power series expansion of the potential energy density (strain energy density) in the Lagrangian contains terms through the third order. These third order terms lead to nonlinear terms in the wave equation. Second, the strains contain nonlinear terms themselves since they represent a finite deformation of the propagation medium. Solution of the nonlinear wave equation yields relationships between the harmonic amplitudes of the distorted ultrasonic wave and the coefficients of the strain energy density expansion (the elastic constants).

I. DEFINITION OF LAGRANGIAN STRAINS

A point in an unstrained solid may be represented by the vector $\vec{a}$. When the solid is strained by application of some stress the point is located by a new vector $\vec{x}$. The point thus undergoes a displacement

$$\vec{u} = \vec{x} - \vec{a} \tag{II.1}$$

when the stress is applied. The vector $\vec{a}$ describes the point in Lagrangian (laboratory) coordinates and the vector $\vec{x}$ describes the same point in Eulerian coordinates (which are fixed in the solid). The strain associated with the deformation of the solid may be described either in Lagrangian or Eulerian coordinates. Since we must make experimental measurements in a laboratory reference frame we shall use Lagrangian coordinates.

Consider two points in the solid in the unstrained state and let the distance $d\ell$ between them be given by

$$d\ell^2 = |d\vec{a}|^2 = da_i^2 \tag{II.2}$$

where Einstein notation (repeated indices are summed) is assumed. The distance between the same two points in the strained state $d\ell'$ is given by

$$d\ell'^2 = |d\vec{x}|^2 = dx_i^2 \ . \tag{II.3}$$

From Eq. (II.1) we may write

$$d\ell'^2 = (da_i + du_i)^2 = (da_i + \frac{\partial u_i}{\partial a_j} da_j)^2 \ . \tag{II.4}$$

From Eqs. (II.2) and (II.4),

$$d\ell'^2 - d\ell^2 = 2\eta_{ij} da_i da_j \tag{II.5}$$

where η_{ij} are the elements of the Lagrangian strain tensor defined by

$$\eta_{ij} = \frac{1}{2}\left(\frac{\partial u_i}{\partial a_j} + \frac{\partial u_j}{\partial a_i} + \frac{\partial u_\ell}{\partial a_i}\frac{\partial u_\ell}{\partial a_j}\right) . \tag{II.6}$$

For small amplitude strains the second order terms in Eq. (II.6) are commonly dropped and the η_{ij} reduce to the form $\frac{1}{2}\left(\frac{\partial u_i}{\partial a_j} + \frac{\partial u_j}{\partial a_i}\right)$ used in linear theory (Green, 1973). However, they are essential in the proper description of the subsequent nonlinear effects.

II. THE EQUATION OF MOTION

The equation of motion in laboratory coordinates can be obtained from Lagrange's equation for a continuous medium (Goldstein, 1968),

$$\frac{d}{dt}\left(\frac{\partial L}{\partial \dot{x}_i}\right) + \left(\frac{d}{da_k}\ \frac{\partial L}{\partial x_i}{\Big/}\partial\left(\frac{\partial}{\partial a_k}\right)\right) + \frac{\partial L}{\partial x_i} = 0 \tag{II.7}$$

where the Lagrangian density L is given by

$$L = \frac{1}{2}\rho_0 \dot{x}_i^2 - \phi(\eta) , \tag{II.8}$$

ρ_0 is the mass density of the unstrained medium, and $\phi(\eta)$ is the strain energy density. It is seen that the strain (and hence the nonlinearity) enters the equation of motion only through the strain energy density.

III. THE STRAIN ENERGY DENSITY AND ELASTIC CONSTANTS

When an elastic body is deformed the agent applying the stress necessarily does work on that body. If we combine the first and second laws of thermodynamics we can write the change in internal energy of the deformed body as

$$dU = TdS - dW \tag{II.9}$$

where U is the internal energy function per unit volume, T is the temperature, S is the entropy and dW is the work done by the agent in deforming the body. Assuming that the applied stress on the body is represented by the stress tensor τ_{ij}, Thurston (1964) showed that Eq. (II.9) can be written as

$$dU = TdS + \frac{1}{\rho_0} \tau_{ij}\, d\eta_{ij} \,. \tag{II.10}$$

Thus, we may consider the internal energy function U to be a function of the entropy S and Lagrangian strains η_{ij}.

If we expand $U(S,\eta_{ij})$ in a power series of the strains we get

$$U(S,\eta_{ij}) = U(S) + \frac{1}{2} \rho_0 \left(\frac{\partial^2 U}{\partial \eta_{ij} \partial \eta_{k\ell}}\right)_S \eta_{ij}\eta_{k\ell}$$

$$+ \frac{1}{3!} \rho_0 \left(\frac{\partial^3 U}{\partial \eta_{ij} \partial \eta_{k\ell} \partial \eta_{mn}}\right)_S \eta_{ij}\eta_{k\ell}\eta_{mn} + \cdots . \tag{II.11}$$

Writing the Helmholtz free energy per unit volume F = U - TS, the differential of F is

$$dF = -SdT + \frac{1}{\rho_0}\tau_{ij}d\eta_{ij} \ . \qquad \text{(II.12)}$$

Hence, we may consider F to be a function of T and η_{ij}, and expand F in a power series analogous to Eq. (II.11),

$$F(T,\eta_{ij}) = F(T) + \frac{1}{2}\rho_0\left(\frac{\partial^2 F}{\partial\eta_{ij}\partial\eta_{k\ell}}\right)\eta_{ij}\eta_{k\ell}$$

$$+ \frac{1}{3!}\rho_0\left(\frac{\partial^3 F}{\partial\eta_{ij}\partial\eta_{k\ell}\partial\eta_{mn}}\right)\eta_{ij}\eta_{k\ell}\eta_{mn} \ . \qquad \text{(II.13)}$$

Brugger (1964), making use of the strain dependence of the thermodynamic state functions U and F, defined the coefficients of the nth order in the power series in Eqs. (II.11) and (II.13) to be the adiabatic and isothermal elastic constants of nth order, respectively. Thus,

$$C^S_{ijk\ell\ldots} = \rho_0\left(\frac{\partial^n U}{\partial\eta_{ij}\partial\eta_{k\ell}\cdots}\right)_S \begin{pmatrix}\text{adiabatic}\\ n \geq 2\end{pmatrix} \qquad \text{(II.14)}$$

and

$$C^T_{ijk\ell\ldots} = \rho_0\left(\frac{\partial^n F}{\partial\eta_{ij}\partial\eta_{k\ell}\cdots}\right)_T \begin{pmatrix}\text{isothermal}\\ n \geq 2\end{pmatrix} \ . \qquad \text{(II.15)}$$

If we equate the strain energy density in Eq. (II.8) to either the internal energy per unit volume U or the Helmholtz free energy per unit volume F, respectively, then the equation of motion [Eq. (II.7)] that results would describe adiabatic or isothermal motion, respectively.

In general, there are 81 second-order and 729 third-order elastic constants. Lattice symmetries of the medium can reduce the number of independent constants so that in isotropic media there are only two independent second-order elastic constants and three third-order elastic constants (Birch, 1947).

Since the Lagrangian strains defined by Eq. (II.6) are symmetric, only six of each set of nine strains are independent. Hence, we may introduce the following contraction of subscript notation (Voigt, 1928):

$$11 \rightarrow 1,\ 22 \rightarrow 2,\ 33 \rightarrow 3,\ 23 \rightarrow 4,\ 13 \rightarrow 5,\ 12 \rightarrow 6\ .$$

If we combine Brugger's definitions of the elastic constants, Voigt's contracted notation, and Birch's study of crystalline symmetries, then the two independent second-order elastic constants for isotropic solids may be written as

$$C_{12},\ C_{44}$$

with

$$C_{11} = C_{12} + 2C_{44}$$

and the three independent third-order constants as

$$C_{111},\ C_{144},\ C_{456}\ .$$

IV. THE ADIABATIC NONLINEAR WAVE EQUATION

If we let the strain energy density in Eq. (II.8) be the internal energy function per unit volume [given by Eq. (II.11)] and substitute Eq. (II.8) into Lagrange's Eq. (II.7) we get

$$\rho_0 \ddot{x}_i - \left\{ \frac{d}{da_k} \frac{\partial U}{\partial \eta_{j\ell}} \frac{\partial \eta_{j\ell}}{\partial x_i / \partial a_k} \right\} = 0 \ . \qquad (II.16)$$

From the definition of strain [Eq. (II.6)] and Eq. (II.1) we may write

$$\frac{\partial \eta_{j\ell}}{\partial x_i / \partial a_k} = \frac{1}{2} \delta_{jk} \left(\frac{\partial x_i}{\partial a_\ell} \right) + \frac{1}{2} \delta_{\ell k} \left(\frac{\partial x_i}{\partial a_j} \right) \ . \qquad (II.17)$$

Hence, the equation of motion becomes

$$\rho_0 \ddot{x}_i = \frac{d}{da_k} \left\{ \frac{\partial U}{\partial \eta_{ik}} + \frac{\partial U}{\partial \eta_{qk}} \frac{\partial u_i}{\partial a_q} \right\} \ . \qquad (II.18)$$

This equation is a general wave equation valid for all directions of propagation and polarizations. Breazeale and Ford (1965) have shown that pure mode propagation of longitudinal waves in cubic crystals occur only in the [100], [110], and [111] crystallographic directions and may occur in any direction for isotropic solids. For any direction in isotropic solids Eq. (II.18) may be written

$$\rho_0 \ddot{u} = C_{11} \frac{\partial^2 u}{\partial a^2} + (3C_{11} + C_{111}) \frac{\partial u}{\partial a} \frac{\partial^2 u}{\partial a^2} \ . \qquad (II.19)$$

Equation (II.19) is the adiabatic equation of motion (and C_{11} and C_{111} are adiabatic elastic constants) since the internal energy function was used for the strain energy density. For the frequency range used in these experiments the use of the internal energy function is justified.

V. SOLUTION TO THE NONLINEAR WAVE EQUATION

Breazeale and Ford (1965) solved the equation of motion [Eq. (II.19)] by assuming an initial sinusoidal disturbance $A_1 \sin\omega t$ at $a = 0$. Their solution may be written for isotropic solids as

$$U = A_1 \sin(ka - \omega t) - \left(\frac{3C_{11} + C_{111}}{8C_{11}}\right) A_1^2 k^2 a \cos 2(ka - \omega t) \tag{II.20}$$

where

A_1 is the amplitude of the fundamental,

k is the propagation constant, $2\pi/\lambda$, and

a is the sample length.

Inspection of Eq. (II.20) reveals that the initially pure sinusoidal disturbance becomes distorted as it propagates through the medium. That is, a wave of frequency 2ω is generated and grows linearly with propagation distance in the sample. It is interesting to note that if one considers a "linear" solid to be one in which no second harmonic is generated, then the necessary condition is that

$$C_{111} = -3C_{11} , \tag{II.21}$$

and <u>not</u> that the third-order elastic constants be zero. So far, no material has been found which satisfies the condition of Eq. (II.21).

VI. THE NONLINEARITY PARAMETER

In Eq. (II.20) the quantities that are measured in the laboratory are the amplitudes of the fundamental and second harmonic at the end of

the sample opposite that at which the initial sinusoidal disturbance is generated. Hence, the coefficients of the trigonometric functions in Eq. (II.20) yield a value A_1 for the fundamental amplitude and

$$A_2 = -\left(\frac{3C_{11} + C_{111}}{8C_{11}}\right) A_1^2 k^2 a \qquad \text{(II.22)}$$

for the second harmonic amplitude. Solving for C_{111} we get

$$C_{111} = -3C_{11}\left(\frac{8}{3}\frac{A_2}{A_1^2}\frac{1}{k^2 a} + 1\right) . \qquad \text{(II.23)}$$

All quantities on the right hand side of this equation can be measured, and C_{111} can be determined.

The quantity

$$\frac{8}{3}\frac{A_2}{A_1^2}\frac{1}{k^2 a} = \beta \qquad \text{(II.24)}$$

in Eq. (II.23) is a significant quantity in this study. If β were zero, then we see that the condition of Eq. (II.21) is satisfied for no second harmonic generation. As we shall see (Chapter III), β is related to the Grüneisen parameter which is a thermodynamic measure of material anharmonicity.

We shall refer to β as the ultrasonic nonlinearity parameter. For isotropic solids β is expressed in terms of the elastic constants as

$$\beta = -\left(\frac{3C_{11} + C_{111}}{3C_{11}}\right) . \qquad \text{(II.25)}$$

CHAPTER III

THE GRÜNEISEN PARAMETER AND ITS RELATION TO THE NONLINEARITY PARAMETER

The parameter β defined in Eq. (II.24) offers a direct measure of material anharmonicity through measurement of elastic nonlinearity of the material structure. However, anharmonicity can be investigated from other measurements. Among them are isothermal compressibility variations as a function of pressure, the thermal expansivity as a function of temperature, and variations of refractive index with temperature (Primak, 1975). Among those investigating anharmonicity from these techniques it has become common to express the results in terms of the Grüneisen parameter γ, defined by

$$\gamma = \frac{\alpha}{K_T C_V} = \frac{\alpha}{K_S C_P} \qquad \text{(III.1)}$$

where α is the thermal volume expansivity, K_T and K_S the isothermal and isentropic compressibilities, respectively, and C_V and C_P the isochoric and isobaric heat capacities, respectively (Grüneisen, 1926). It is the purpose of this chapter to show the relation of the Grüneisen parameter to the nonlinearity parameter β.

I. RELATION BETWEEN THE STATISTICAL MECHANICAL MODEL OF A SOLID AND THE THERMODYNAMIC STATE FUNCTIONS

A solid can be represented as the sum of two entities: an array of atoms at rest in their mean positions with static potential energy ϕ_o

plus an assembly of lattice vibrations represented as a set of weakly interacting but distinguishable simple harmonic oscillators. The set of simple harmonic oscillators may be designated by a branch index p, wave vector $\vec{q}$, frequency $\omega(p,\vec{q})/2\pi$, and energies

$$E_{n(p,\vec{q})} = [n(p,\vec{q}) + \frac{1}{2}]h\omega(p,\vec{q}) \qquad \text{(III.2)}$$

where $n(p,\vec{q}) = 0, 1, 2, 3, \ldots$ and h is Planck's constant divided by 2π. The partition function for such a system is (Slater, 1939)

$$Z = e^{\frac{-\phi_o}{kT}} \sum_{p\vec{q}\ n(p,\vec{q})} e^{\frac{-E_{n(p,\vec{q})}}{kT}} . \qquad \text{(III.3)}$$

where k is the Boltzmann constant and T is the temperature.

The relation between the statistical mechanical model of a solid and the thermodynamic state functions U (internal energy) and F (Helmholtz free energy) is given by (Hill, 1962)

$$U = \frac{kT^2}{Z}\left(\frac{\partial Z}{\partial T}\right)_V = kT^2\left(\frac{\partial \ell nZ}{\partial T}\right)_V \qquad \text{(III.4)}$$

and

$$F = -kT\ell nZ . \qquad \text{(III.5)}$$

II. THE "STRAIN" GENERALIZED GRÜNEISEN PARAMETERS

The thermal expansivity α given in Eq. (III.1) may be generalized to tensorial form by (Thurston, 1964)

$$\alpha_{jk} = \left(\frac{\partial \eta_{jk}}{\partial T}\right)_{\tau} \tag{III.6}$$

where η_{jk} are components of the Lagrangian strain tensor, T is the temperature, and the subscript τ means the thermal strain derivative is evaluated at constant stress. In terms of the Helmholtz free energy we may write (Brugger and Fritz, 1967)

$$\alpha_{jk} = - \sum_{rs} S^{T}_{jkrs} \left(\frac{\partial^2 F/V}{\partial T \partial \eta_{rs}}\right) \tag{III.7}$$

where the S^{T}_{jkrs} are the isothermal elastic compliance coefficients and V is the volume of the solid.

If we assume that ϕ_o and $\omega(p,\vec{q})$ depend on temperature only through the lattice dimensions (quasiharmonic approximation) (Liebfried and Ludwig, 1961), then from Eqs. (III.3) and (III.5) we may write Eq. (III.7) in the form

$$\alpha_{jk} = \sum_{rs} \sum_{p\vec{q}} S^{T}_{jkrs} \gamma_{rs}(p,\vec{q}) C(p,\vec{q}) \tag{III.8}$$

where the strain generalized Grüneisen parameters, $\gamma_{rs}(p,\vec{q})$, are defined by

$$\gamma_{rs}(p,\vec{q}) = - \left[\frac{1}{\omega(p,\vec{q})} \left(\frac{\partial \omega(p,\vec{q})}{\partial \eta_{rs}}\right)_{T}\right]_{\eta=0} . \tag{III.9}$$

These strain generalized Grüneisen parameters are indirectly dependent on temperature through the strains η_{rs}. The $C(p,\vec{q})$ are the modal heat capacities given by

$$C(p,\vec{q}) = \frac{k\left(\frac{\hbar\omega(p,\vec{q})}{kT}\right)^2 e^{\frac{\hbar\omega(p,\vec{q})}{kT}}}{\left(e^{\frac{\hbar\omega(p,\vec{q})}{kT}} - 1\right)^2} . \qquad \text{(III.10)}$$

They are directly temperature dependent.

III. THE "VOLUME" GENERALIZED GRÜNEISEN PARAMETERS

The thermal expansivity α may be expressed in terms of the tensorial α_{jk} by

$$\alpha = \sum_j \alpha_{jj} . \qquad \text{(III.11)}$$

Substituting Eq. (III.8) into Eq. (III.11) gives

$$\alpha = \sum_{p\vec{q}} \left\{ \sum_j \sum_{rs} S^T_{jjrs}\, \gamma_{rs}(p,\vec{q}) \right\} C(p,\vec{q}) . \qquad \text{(III.12)}$$

If we define

$$\gamma(p,\vec{q}) = \frac{1}{K_T} \sum_j \sum_{rs} S^T_{jjrs}\, \gamma_{rs}(p,\vec{q}) \qquad \text{(III.13)}$$

where K_T is the isothermal compressibility and

$$\gamma(p,\vec{q}) = -\frac{V}{\omega(p,\vec{q})} \left\{ \frac{\partial\omega(p,\vec{q})}{\partial V} \right\}_T \qquad \text{(III.14)}$$

then Eq. (III.12) may be written as

$$\alpha = K_T \sum_{p\vec{q}} \gamma(p,\vec{q})C(p,\vec{q}) \ . \qquad \text{(III.15)}$$

Equation (III.15) is the form for α given by Slater (1939) with $\gamma(p,\vec{q})$ being defined by Eq. (III.14). To distinguish the $\gamma(p,\vec{q})$ from the strain generalized Gruneisen parameter $\gamma_{rs}(p,\vec{q})$ of Eq. (III.9) we shall call the $\gamma(p,\vec{q})$ of Eq. (III.14) the volume generalized Grüneisen parameters. Equation (III.13) then gives the relation between the two parameters.

IV. THE GRÜNEISEN PARAMETER AND ITS RELATION TO THE GENERALIZED GRÜNEISEN PARAMETERS

Substituting Eq. (III.15) into Eq. (III.1) gives

$$\gamma = \frac{\sum_{p,\vec{q}} \gamma(p,\vec{q})C(p,\vec{q})}{\sum_{p,\vec{q}} C(p,\vec{q})} \qquad \text{(III.16)}$$

where we have defined

$$C_V = \sum_{p,\vec{q}} C(p,\vec{q}) \ . \qquad \text{(III.17)}$$

Thus, from Eq. (III.16) the Grüneisen parameter γ is equal to a weighted average of the volume generalized Gruneisen parameter $\gamma(p,\vec{q})$. The weighting functions are simply the modal heat capacities $C(p,\vec{q})$.

Substituting Eq. (III.13) into Eq. (III.16) gives the dependence of the Grüneisen parameter on the strain generalized Grüneisen parameter,

$$\gamma = \frac{1}{K_T} \frac{\sum_{\vec{p},\vec{q}} \sum_{j} \sum_{rs} S^{T}_{jjrs} \gamma_{rs}(p,\vec{q}) C(p,\vec{q})}{\sum_{p,\vec{q}} C(p,\vec{q})} . \qquad \text{(III.18)}$$

V. CONTINUUM MODELS AND RESULTING EXPRESSIONS FOR THE GRÜNEISEN PARAMETER

Until now no particular model has been assumed to describe the frequency distribution of the simple harmonic oscillators. The introduction of a frequency distribution has the effect of assigning relative "weights" to the modal heat capacities to reflect the relative number of independent simple harmonic oscillators in a particular mode. This in turn assigns relative "weights," via the modal heat capacities, to the Grüneisen parameter γ.

The continuum model is introduced through the following assumption (Brugger and Fritz, 1967):

1. The excitation of optic modes is neglected so that the branch index p takes on only the values 1, 2, 3 to reflect the longitudinal and two transverse acoustic branches.
2. The acoustic modes obey the Debye frequency distribution function (per unit volume)

$$q(p,\vec{q})dqd\Omega = \frac{1}{(\pi)^{-3}} q^2 dqd\Omega . \qquad \text{(III.19)}$$

3. The maximum value of q along any direction equals the Debye radius

$$q_D = \left(\frac{6\pi^2}{V_o}\right)^{1/3} \qquad \text{(III.20)}$$

where V_o is the volume of the primitive cell of the solid. The volume of the Debye sphere equals that of the first Brillouin zone.

4. The acoustic modes are either nondispersive (Debye model) or they obey the sinusoidal dispersion relation (Born-von Karman model)

$$\frac{\omega}{\omega_{max}} = \sin\left(\frac{\pi}{2}\frac{q}{q_D}\right) . \qquad \text{(III.21)}$$

5. The <u>strain</u> generalized Grüneisen parameters and the <u>volume</u> generalized Grüneisen parameters are independent of wave number (frequency) in both models.

The basic difference between the dispersive and nondispersive models is that the Born-von Karman model assigns a greater "weight" to the low-frequency acoustic modes than does the Debye model.

With these assumptions Eq. (III.16) becomes (Brugger and Fritz, 1967):

$$\gamma = \frac{\sum_p \int d\Omega \gamma(p,\hat{N}) C(p,\hat{N})}{\sum_p \int d\Omega C(p,\hat{N})} \qquad \text{(III.22)}$$

where

$$C(p,\hat{N}) = \left(\frac{q_D}{2\pi}\right)^3 \int_0^1 d\xi \, \frac{\xi^2 Q^2 e^Q}{(e^Q - 1)^2} \qquad \text{(III.23)}$$

and

$$\hat{N} = \frac{\vec{q}}{|\vec{q}|} . \qquad \text{(III.24)}$$

For the Debye model

$$Q_{\text{Debye}}(p,\hat{N},\xi) = \left(\frac{\Theta(p,\hat{N})}{T}\right)\xi \quad . \tag{III.25}$$

For the Born-Von Karman model

$$Q_{\text{Born}}(p,\hat{N},\xi) = \frac{2}{\pi}\left(\frac{\Theta(p,\hat{N})}{T}\right)\sin\left(\frac{\pi}{2}\xi\right) \quad . \tag{III.26}$$

In both models

$$\Theta(p,\hat{N}) = \left(\frac{hq_D}{k}\right) S(p,\hat{N}) \tag{III.27}$$

is the characteristic temperature of the mode specified by p and $\hat{N}$, and

$$S(p,\hat{N}) = \left(\frac{\partial\omega(p,\vec{q})}{\partial q}\right)_{q=0} \tag{III.28}$$

is the acoustical wave speed in the solid.

In terms of the modal characteristic temperatures the Debye temperature Θ is given by

$$\frac{1}{\Theta^3} = \frac{1}{12\pi}\sum_p \int \frac{d\Omega}{[\Theta(p,\hat{N})]^3} \quad . \tag{III.29}$$

VI. THE RELATION OF GENERALIZED GRÜNEISEN PARAMETERS TO ELASTIC CONSTANTS

Equation (III.28) implies that for the Debye model the frequencies are related for any state of strain to the wave speed and some dimension L of the solid by (Brugger, 1965):

$$\omega(p,\hat{q}) = \frac{S(p,\hat{N})}{L} = \frac{W(p,\hat{N})}{L_o} \qquad \text{(III.30)}$$

where $W(p,\hat{N})$ is the wave speed referred to the natural or unstrained dimension L_o. Hence, Eq. (III.9) may be written

$$\gamma_{rs}(p,\hat{N}) = -\frac{1}{2w(p,\hat{N})}\left[\frac{\partial \rho_o W^2(p,\hat{N})}{\partial \eta_{rs}}\right]_{T,\eta=0} \qquad \text{(III.31)}$$

where

$$w(p,\hat{N}) = [\rho_o W^2(p,\hat{N})]_{\eta=0} \qquad \text{(III.32)}$$

and ρ_o is the density of the unstrained solid.

Thurston and Brugger (1964) have shown that $\rho_o W^2$ in a homogeneously deformed solid is given by

$$\rho_o W^2(p,\hat{N})U_u = w_{uv}U_v \qquad \text{(III.33)}$$

where

$$w_{uv} = [\delta_{uv}\bar{\tau}_{mn} + (\delta_{vw} + 2\bar{\eta}_{vw})\bar{C}^S_{munw}]N_m N_n \ . \qquad \text{(III.34)}$$

Summation over repeated indices (Einstein notation) is implied in expressions (III.33) and (III.34) and succeeding equations. τ represents the applied stress and the C's are second-order elastic constants. The bar over the symbols indicates evaluation of the quantity in the deformed state. $\hat{N}$ gives the direction of wave propagation and $\hat{u}$ is a unit vector along the direction of polarization appropriate to p. If the strain derivatives of

Eq. (III.33) are evaluated at zero strain, the strain generalized Grüneisen parameters may be written as

$$\gamma_{rs}(p,\hat{N}) = -\frac{1}{2w(p,\hat{N})}\left[2w(p,\hat{N})U_rU_s + (C_{rsmn} + C_{rskmunv}U_uU_v)N_mN_n\right] \qquad \text{(III.34a)}$$

where

$$w(p,\hat{N}) = C_{munv}N_mN_nU_uU_v \ . \qquad \text{(III.35)}$$

Equation (III.34a) is the expression relating the strain generalized Grüneisen parameters to the elastic constants.

The volume generalized Gruneisen parameters in terms of the elastic constants may be obtained by substituting Eq. (III.34a) into Eq. (III.13).

$$\gamma(p,\hat{N}) = -\frac{1}{2K_Tw(p,\hat{N})}S_{jjrs}\left[2w(p,\hat{N})U_rU_s + (C_{rsmn} + C_{rsmunv}U_uU_v)N_mN_n\right] \qquad \text{(III.36)}$$

(Einstein notation).

VII. THE RELATION OF THE GRÜNEISEN PARAMETERS TO THE NONLINEARITY PARAMETER

In an isotropic solid all directions are equivalent. Hence, we can simplify Eq. (III.34a) for the strain generalized Grüneisen parameters by assuming $N_1=1$, $N_2=N_3=0$, and $U_1=1$, $U_2=U_3=0$, for the propagation of a pure mode longitudinal ultrasonic wave in an isotropic solid.

Equation (III.34a) then gives for the tensor element (r=1, s=1) for all longitudinal modes $(p_\ell,\hat{N})$

$$\gamma_{11}(p_\ell,\hat{N}) = - \frac{3C_{11} + C_{111}}{2C_{11}} \qquad \text{(III.37)}$$

where the notation p_ℓ is used to emphasize the longitudinal acoustic mode. From Eq. (II.25) of Chapter II and Eq. (III.37), the relation between $\gamma_{11}(p_\ell,\hat{N})$ and the ultrasonic nonlinearity parameter β is

$$\gamma_{11}(p_\ell,\hat{N}) = \frac{3}{2}\beta \ . \qquad \text{(III.38)}$$

It is to be emphasized that there are nine strain generalized Grüneisen parameters for each mode $(p_\ell,\hat{N})$ corresponding to the nine tensor indices (r,s). For the isotropic solid the other tensor elements may be expressed for all longitudinal modes $(p_\ell,\hat{N})$ as

$$\gamma_{22}(p_\ell,\hat{N}) = \gamma_{33}(p_\ell,\hat{N}) = - \frac{C_{12} + C_{112}}{2C_{11}} \ , \qquad \text{(III.39)}$$

and

$$\gamma_{ij}(p_\ell,\hat{N}) = 0 \quad \text{for } i \neq j \ . \qquad \text{(III.40)}$$

Hence, the other tensor elements of the strain generalized Grüneisen parameter do not give such a simple relation to the nonlinearity parameter β. The transverse modes $(p_t,\hat{N})$ yield a different set of nine strain generalized Grüneisen parameters.

Using the expressions for the longitudinal mode strain generalized Gruneisen parameters [Eqs. (III.37), (III.39), and (III.40)], we obtain

from Eq. (III.13) the volume generalized Grüneisen parameters for the longitudinal modes $(p_\ell,\hat{N})$ in terms of the elastic constants,

$$\gamma(p_\ell,\hat{N}) = -\frac{1}{2}\beta - \left(\frac{C_{12} + C_{112}}{3C_{11}}\right) . \qquad \text{(III.41)}$$

Using the relationships among the second- and third-order elastic constants for an isotropic solid as given by Toupin and Bernstein (1961) we get

$$\gamma(p_\ell,\hat{N}) = \frac{2}{3}\left\{1 + \frac{C_{44} + 2C_{144} + 4C_{456}}{C_{11}}\right\} - \frac{3}{2}\beta . \qquad \text{(III.42)}$$

Thus, the volume generalized Grüneisen parameters in the longitudinal modes $(p_\ell,\hat{N})$ contain elastic constants that are not measured by the harmonic generation technique. However, one component, $\frac{3}{2}\beta$, is measured directly.

The transverse mode $(p_t,\hat{N})$ volume generalized Grüneisen parameters are obtained from the transverse mode strain generalized Grüneisen parameters in the manner described above for the longitudinal mode parameters. They contain terms involving elastic constants other than C_{11} *and* C_{111} *also. Thus, the* Grüneisen parameter γ will also contain such terms.

For an isotropic solid Eq. (III.22) simplifies to

$$\gamma = \frac{\gamma(p_\ell,\hat{N})\, C_\ell + 2\gamma(p_t,\hat{N})\, C_t}{C_\ell + 2\, C_t} \qquad \text{(III.43)}$$

where $\gamma(p_\ell,\hat{N})$ is the longitudinal mode volume generalized Gruneisen parameter given by Eq. (III.42), $\gamma(p_t,\hat{N})$ is the transverse mode volume

generalized Grüneisen parameter, and C_ℓ and C_t are the weighting functions given by Eq. (III.23).

For anisotropic solids the calculation of the strain and volume generalized Grüneisen parameters as well as the Grüneisen parameter γ is much more complicated. For anisotropic solids each longitudinal mode specified by a particular value of the set $(p_\ell,\hat{N})$ will, in general, have nine different strain generalized Gruneisen parameters. This is in contrast to the isotropic solid in which all values of the set $(p_\ell,\hat{N})$ have the same set of nine strain generalized Grüneisen parameters. The same considerations apply to the difference between isotropic and anisotropic solids for the transverse modes $(p_t,\hat{N})$.

The volume generalized Grüneisen parameters are related to the strain generalized Grüneisen parameters through Eq. (III.13). It is seen that in an anisotropic solid the longitudinal and transverse components of the volume generalized Grüneisen parameter cannot be represented by values which are independent of particular values of mode specification $(p_\ell,\hat{N})$ or $(p_t,\hat{N})$, as was done for the case of isotropic solids. Hence, calculation of the Grüneisen parameter γ cannot be done with a simple expression as Eq. (III.43). For anisotropic solids Eq. (III.22) must be used. In addition, for anisotropic solids the calculation of the modal specific heat "weighting" functions [Eq. (III.23)] involves calculation of directional dependent modal characteristic temperatures. This further complicates the problem for calculating anisotropic Grüneisen parameters.

Finally, it is of interest to note that for the [1,0,0] direction in a cubic crystal the longitudinal mode strain generalized Grüneisen parameter specified by tensor component [r=1, s=1] may be written

$$\gamma_{11}(p_\ell;\ 1,0,0) = -\frac{3C_{11} + C_{111}}{2C_{11}} = \frac{3}{2}\beta\ . \qquad \text{(III.44)}$$

This is identical to the value given in Eq. (III.37) for all longitudinal modes of an isotropic solid for the [r=1, s=1] component. However, as pointed out above, Eq. (III.44) gives but one of an infinite number (one for each direction) of [r=1, s=1] strain generalized Grüneisen parameters which ultimately must be used (together with other (r,s) components) in the calculation of the Grüneisen parameter γ.

VIII. THE TEMPERATURE DEPENDENCE OF THE GRÜNEISEN PARAMETERS

It was assumed in the expression relating the thermal expansivity tensor α_{jk} to the Helmholtz free energy F [Eq. (III.7)] that if ϕ_o (the static potential energy of the lattice system) and $\omega(p,\vec{q})$ (the frequencies of the simple harmonic oscillators) were directly independent of temperature, then the α_{jk} could be expressed in terms of tensor entities called the strain generalized Grüneisen parameters. These entities are also directly independent of temperature from their definition [Eq. (III.9)], and depend on temperature only through the lattice dimensions (i.e., the γ_{jk} are strain dependent). The introduction of the Debye model eliminated the frequency dependence of the strain generalized Grüneisen parameters and that allowed for the expression of

the strain generalized Grüneisen parameters exclusively in terms of the elastic constants. Hence, the strain generalized Grüneisen parameters are independent of temperature to the extent that the Debye model is accurate and that the combinations of elastic constants representing a particular mode (p,N) and tensor component (r,s) is independent of temperature.

It has been shown that the $\gamma_{11}(p_\ell,\hat{N})$ strain generalized Gruneisen parameter of an isotropic solid is equal to $\frac{3}{2}\beta$, where β is the ultrasonic nonlinearity parameter. Since β is measured directly in the harmonic generation technique, the variation of $\gamma_{11}(p_\ell,\hat{N})$ with temperature can be measured directly. Measurements of the other $\gamma_{rs}(p_\ell,\hat{N})$ and all $\gamma_{rs}(p_t,\hat{N})$ for isotropic solids must be obtained from other measurements of the temperature dependence of the second- and third-order elastic constants.

The volume generalized Grüneisen parameters are also directly independent of temperature since they involve sums of the strain generalized Grüneisen parameters weighted by isothermal compressibility tensor components S_{jjrs}. No direct measurement of any volume generalized Grüneisen parameter is possible with the harmonic generation technique since all such parameters involve terms other than C_{11} and C_{111} (isotropic solids).

Since the volume generalized Grüneisen parameters are directly independent of temperature, the Grüneisen parameter γ can depend directly on temperature only through the modal specific heats as shown in Eq. (III.22) [Eq. (III.43) for isotropic solids]. The modal specific

heats can be calculated (usually numerically) as functions of temperature and the temperature dependence of all the elastic constants can be measured experimentally by combining the harmonic generation technique with other techniques [for example, an ultrasonic beam mixing technique (Dunham and Huntington, 1970)]. Hence, all the factors in the right hand side of Eqs. (III.22) or (III.43) can be measured or calculated as functions of temperature, and the Grüneisen parameter calculated.

The Grüneisen parameter can also be determined experimentally from other measurements [Eq. (III.1)]. Comparing the theoretically determined value for the Gruneisen parameter [Eqs. (III.22) or (III.43) and the experimentally determined value [Eq. (III.1)] gives a direct check of the validity of the Debye theory for a particular solid.

Although some comparisons between the theoretically and experimentally determined Grüneisen parameters have been made for various solids (Gerlich, 1975; Brugger and Fritz, 1967; Schuele and Smith, 1963; Sheard, 1958), the results are largely inconclusive because of the lack of experimental data on the temperature dependence of the third-order elastic constants. This lack of information provided motivation for the measurements of the temperature dependence of third-order elastic constants reported in this dissertation.

CHAPTER IV

APPARATUS, PROCEDURES, AND SAMPLES

I. EXPERIMENTAL CONSIDERATIONS

The determination of the adiabatic nonlinearity parameters of the solid samples was made by measuring both the amplitudes of the longitudinal wave introduced into the specimen and the amplitude of the generated second harmonic component. The fundamental frequency was chosen to be 30 MHz. Such a choice represents a compromise between the fact that the second harmonic amplitude A_2 increases as the square of the frequency and the fact that attenuation and effects of nonparallelism of the sample surfaces also increases with frequency. To avoid diffraction effects it was desirable to work above 10 MHz (Gauster, 1966). For the samples used in these measurements a 30 MHz fundamental frequency provided an adequate signal-to-noise ratio while introducing errors due to attenuation that were negligible relative to other sources of error.

A pulse-echo technique was used in all measurements to eliminate complicated interference effects. A 60 Hz pulse repetition rate was chosen to minimize heating of the samples and to reduce ground loops.

Since only in the limit of infinitesimal fundamental amplitude is the second harmonic related in amplitude to the fundamental according to a simple integral power law (Thurston and Shapiro, 1967), the fundamental amplitude was kept as low as possible consistent with a useful signal-to-noise ratio.

II. ABSOLUTE AMPLITUDE MEASUREMENTS OF THE ULTRASONIC WAVE HARMONICS

The amplitudes of the fundamental and generated second harmonic waves were measured absolutely in each sample at room temperature. At all other temperature points the amplitudes were measured relative to the room temperature values. From a knowledge of the absolute wave amplitudes, the third-order elastic constant C_{111} is calculated from Eq. (II.23) as

$$C_{111} = -\left\{\frac{8}{3}\frac{A_2}{A_1^2 k^2 a} + 1\right\} 3\, C_{11} \qquad \text{(IV.1)}$$

where C_{11} is calculated from velocity measurements.

Room Temperature Apparatus

The absolute amplitude measurements were made with the room temperature apparatus as shown in Figure IV.1. A cross-sectional view of the apparatus is shown in Figure IV.2. An ultrasonic signal is generated by an X-cut piezoelectric quartz transducer, propagates through the sample, and is detected at the other end by an air-gap capacitive receiver. The capacitive receiver is a parallel plate capacitor consisting of an electrically conducting sample face and 0.400 inch diameter electrode recessed approximately 7 microns from the sample surface. A dc bias of the order of 140 volts is applied across the gap through a large resistor (approximately 1 MΩ) to keep the current through the detector low in case of electrical arc over.

In order to make accurate amplitude measurements of the ultrasonic waves, provision is made to place a substitutional signal on the receiver

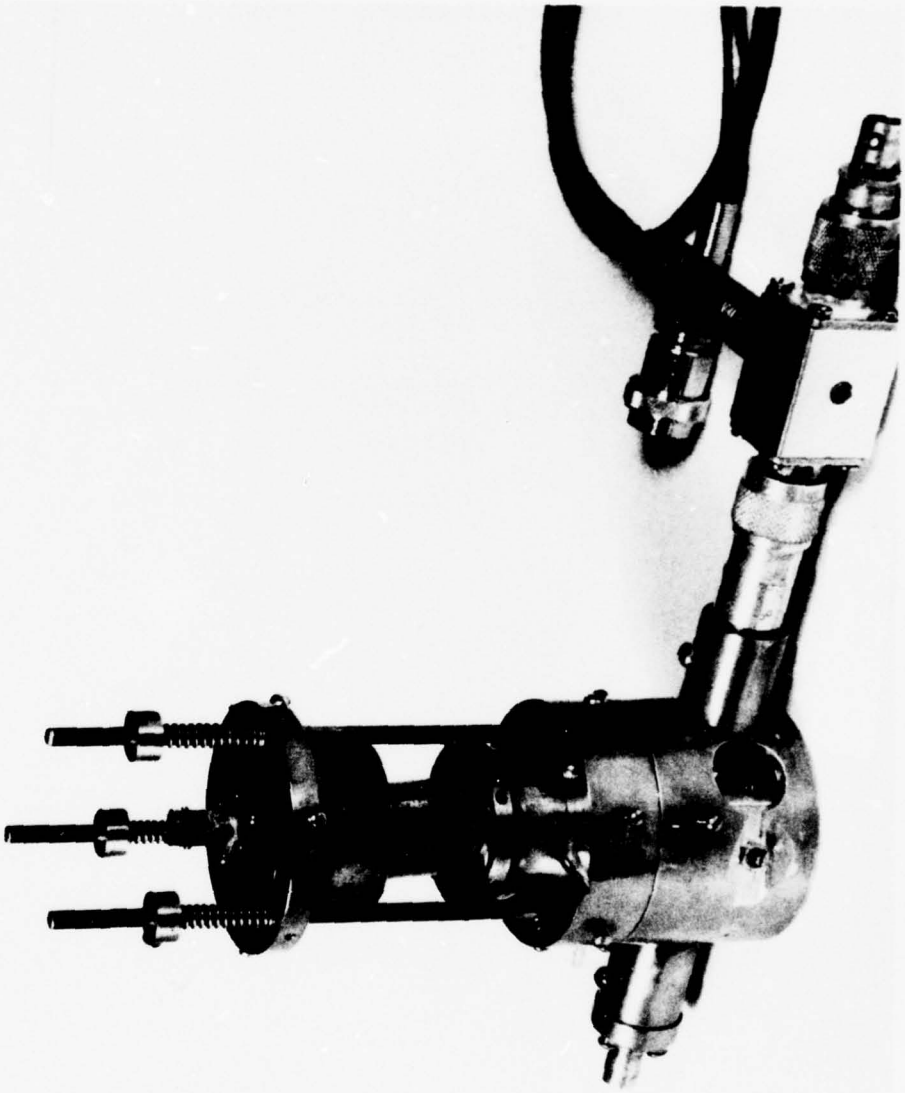

Figure IV.1. The Room Temperature Apparatus.

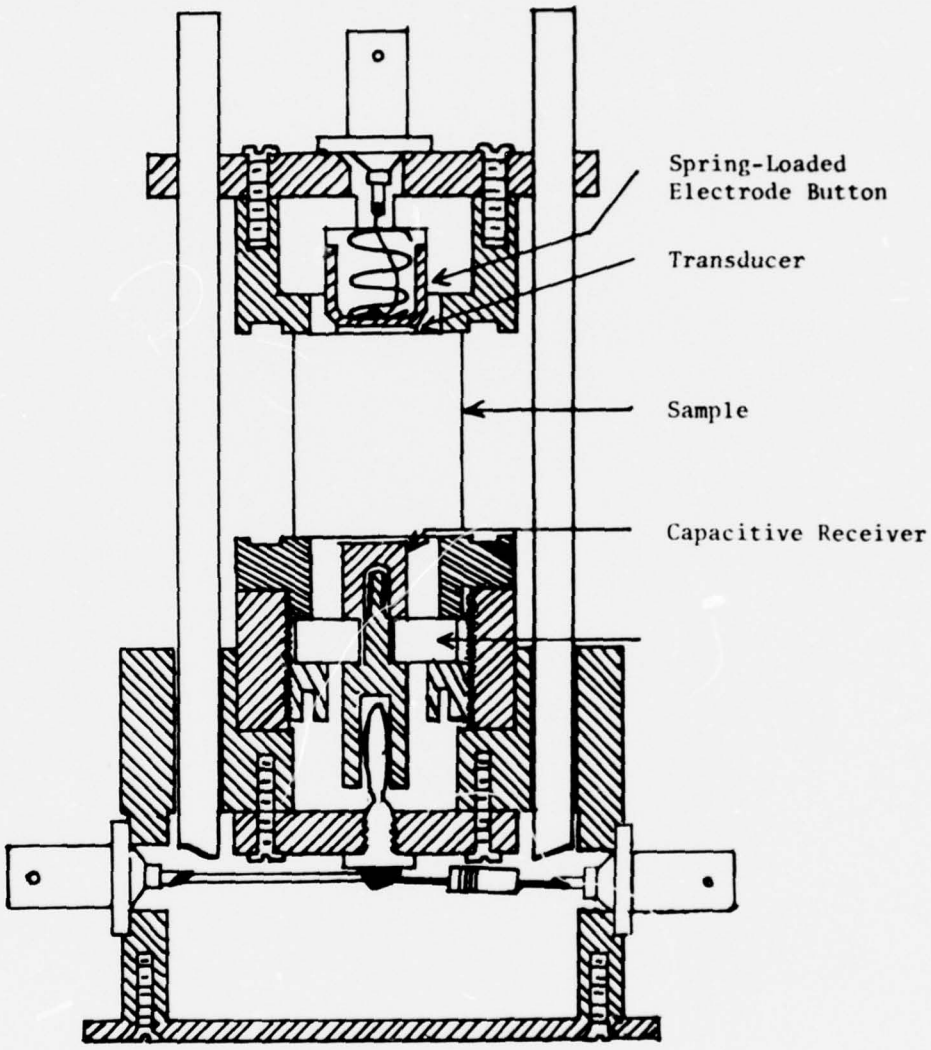

Figure IV.2. Cross Sectional View of the Room Temperature Apparatus.

through a large resistor (approximately 10 KΩ) between the receiver and the substitutional signal source.

Room Temperature Calibration and Procedure

The absolute determination of the fundamental and second harmonic ultrasonic wave amplitudes is made with the apparatus arrangement shown in the block diagram of Figure IV.3.

A cw signal from a stable VFO is used to drive a gated amplifier. The resulting pulsed 30 MHz signal is passed through a power amplifier designed to deliver full power at any load impedance. The output from the power amplifier is then passed through a 30 MHz bandpass filter which insures the spectral purity of the ultrasonic wave, even when the transducer is driven off resonance.

At the opposite end of the sample the ultrasonic wave generates an electrical signal in the capacitive receiver. This signal is sent through either a 30 MHz or 60 MHz bandpass amplifier. From there the signal is taken to a boxcar integrator. The boxcar integrator selects a portion of the first echo and gives an output signal proportional to the time average of that portion of the echo.

After recording the magnitude of the fundamental and second harmonic outputs, a continuous (cw) substitutional signal is introduced at the capacitive receiver. The 30 MHz filter used previously to insure the spectral purity of the gated signal is now used to filter the 30 MHz cw signal. The 60 MHz cw substitutional signal is derived by passing the 30 MHz cw signal through a ring bridge mixer and filtering the output with a 60 MHz bandpass filter. The magnitudes of the two signals are

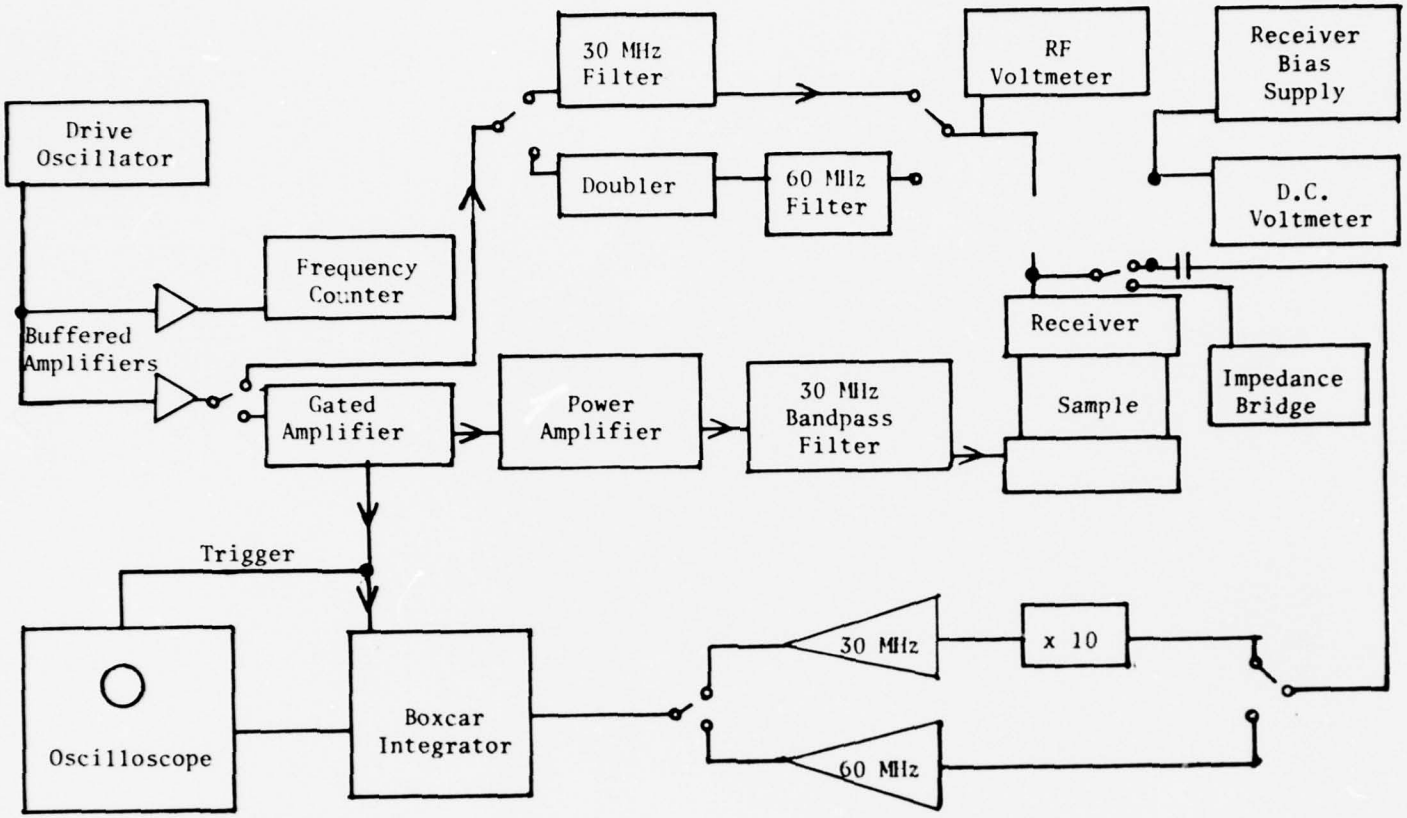

Figure IV.3. Block Diagram for the Room Temperature Nonlinearity Measurements.

adjusted to give the same output signals as recorded in the pulse measurements. The cw signals are then measured with an rf voltmeter, and the amplitudes of the fundamental and second harmonic wave components are calculated.

The equivalent circuit for making the ultrasonic wave amplitude calculations is shown in Figure IV.4. A Norton equivalent circuit is used to represent the ac equivalent capacitive receiver circuit. The "switch" S_1 is opened by turning off the ultrasonic signal to the receiver. "Switch" S_2 is closed by connecting a signal generator to the apparatus.

It has been shown (Peters, 1968) that the Thevenin equivalent circuit of the capacitive receiver is given as a voltage

$$V = \frac{2\ AV_b}{S_0} \qquad (IV.2)$$

feeding the load resistance R (amplifier impedance) through a capacitance of value C_D, the quiescent receiver capacitance. In the above equation, A is the amplitude of the ultrasonic wave under consideration, V_b is the capacitive receiver bias voltage (140 volts in these experiments), and S_0 is the receiver gap spacing.

Since the receiver voltage is related to the receiver current by $i_D = V\omega C_D$ where ω is the angular frequency of the ultrasonic wave, the Norton equivalent circuit (Bains, 1974) of the detector is a current

$$i_D = \frac{2AV_b\omega C_D}{S_0} \qquad (IV.3)$$

in parallel with the resistance R and receiver capacitance C_D as shown in Figure IV.4. The substitutional signal source is represented in

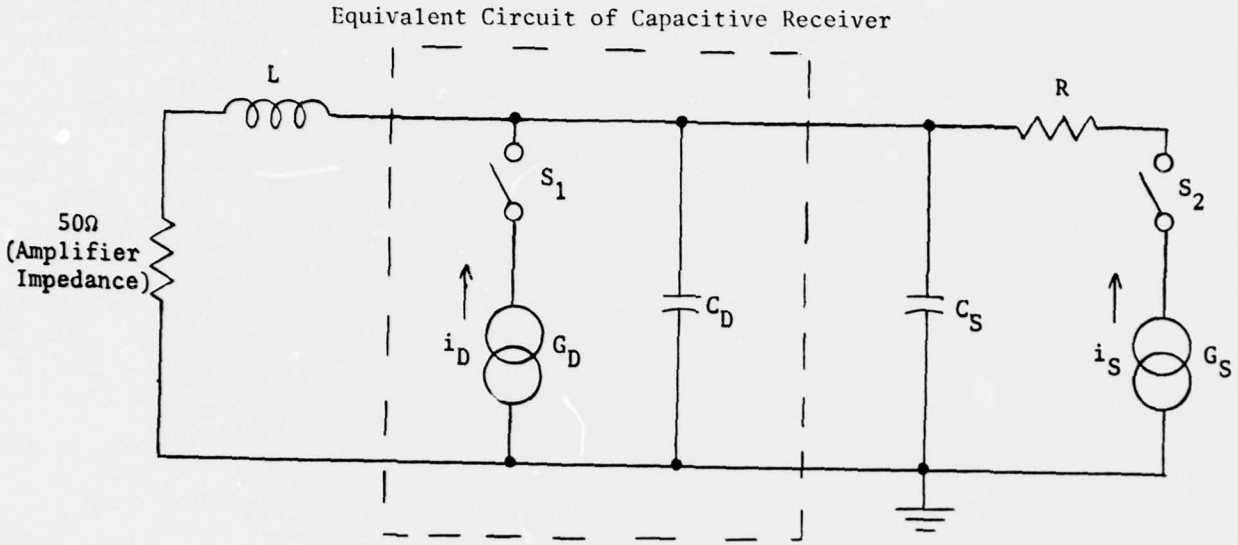

Figure IV.4. Equivalent Circuit of the Room Temperature Apparatus for Absolute Amplitude Measurements.

Figure IV.4 as the current generator G_S. When the magnitude of this current source is adjusted to give the same output from the amplifier as the pulsed ultrasonic signal, i_S is equal to i_D. It is then a matter of measuring i_S to find the ultrasonic wave amplitude from Eq. (IV.3).

Since voltages are generally much easier to measure than currents, i_S is calculated from measurement of the substitutional source voltage and knowledge of the impedance through which the current flows. The inductance L shown in Figure IV.4 is the inductance of the wire leading from the detector to the BNC connector (see Figure IV.2, page 35) and the capacitance C_S is the lumped stray capacitance of the receiver.

At the frequencies used in these experiments the resistor R between the substitutional source and the receiver does not behave as a pure resistance. Hence, the impedance of the resistor must be measured at each frequency used. The equivalent circuit for measurement of the resistor impedance is shown in Figure IV.5.

The sample, bottom plate, and detector assembly are removed from the apparatus and 50Ω terminators are placed on the "signal in" and "signal out" BNC connectors. A cw signal generator is connected to the "signal in" terminator designated as point 1 in Figure IV.5. Probes A and B (with isolator tips) of a vector voltmeter (Hewlett-Packard Model 8405A) are placed at point 1, the phase angle between the signals entering the probes are zeroed and the signal amplitudes are measured. Probe B of the vector voltmeter is then placed at point 2 while leaving probe A at point 1. The signal generator is readjusted to give the original reading for channel A and the amplitude of the B channel and

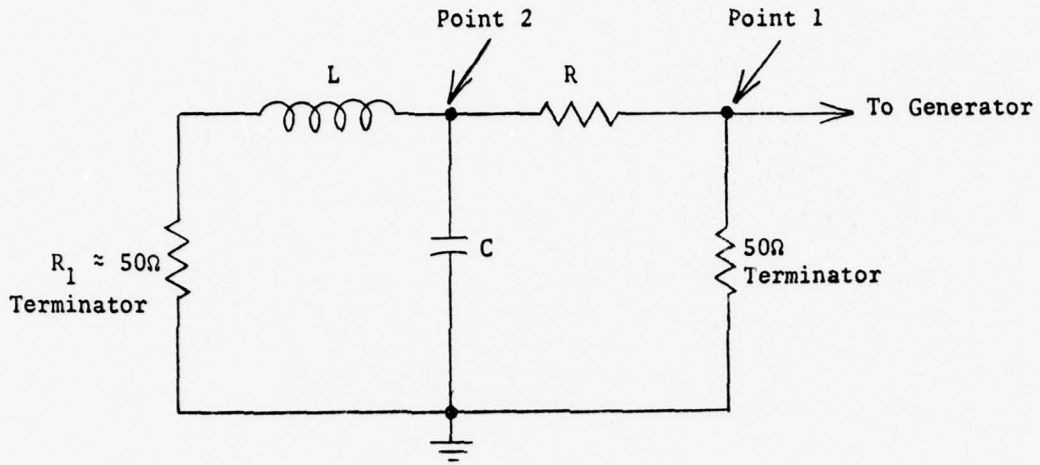

Figure IV.5. Equivalent Circuit of the Room Temperature Apparatus for the Measurement of the Impedance of R.

the phase angle between the channels are recorded. The impedance of the resistor R is then given by

$$Z = \left[j\omega C + \frac{1}{R_1 + j\omega L}\right]^{-1} \frac{V_{B1} - V_{B2}e^{j\phi}}{V_{B2}e^{j\phi}} \qquad \text{(IV.4)}$$

where V_{B1} is the signal amplitude measured by probe B at point 1, V_{B2} is the amplitude measured by probe B at point 2, and ϕ is the phase angle between V_{B1} and V_{B2}. L is the inductance mentioned previously, ω is the angular frequency of the cw input signal, R_1 is the measured resistance of the "signal out" 50Ω terminator, C is the stray capacitance at point 2 (including the probe tip capacitance), and $j^2 = -1$.

The substitutional current is calculated from

$$i_S = \frac{V_S}{Z + \left[j\omega(C_D + C_S) + \frac{1}{50 + j\omega L}\right]^{-1}} \qquad \text{(IV.5)}$$

where V_S is the voltage across the current generator G_S (Figure IV.4, page 39).

III. RELATIVE AMPLITUDE MEASUREMENTS OF THE ULTRASONIC WAVE HARMONICS

The Cryogenic Apparatus

The apparatus used to make the relative ultrasonic wave amplitude measurements basically consists of a transducer driver assembly, a sample holder, and an air-gap capacitive receiver enclosed in a stainless steel can as shown in Figure IV.6. This can is surrounded by another can so

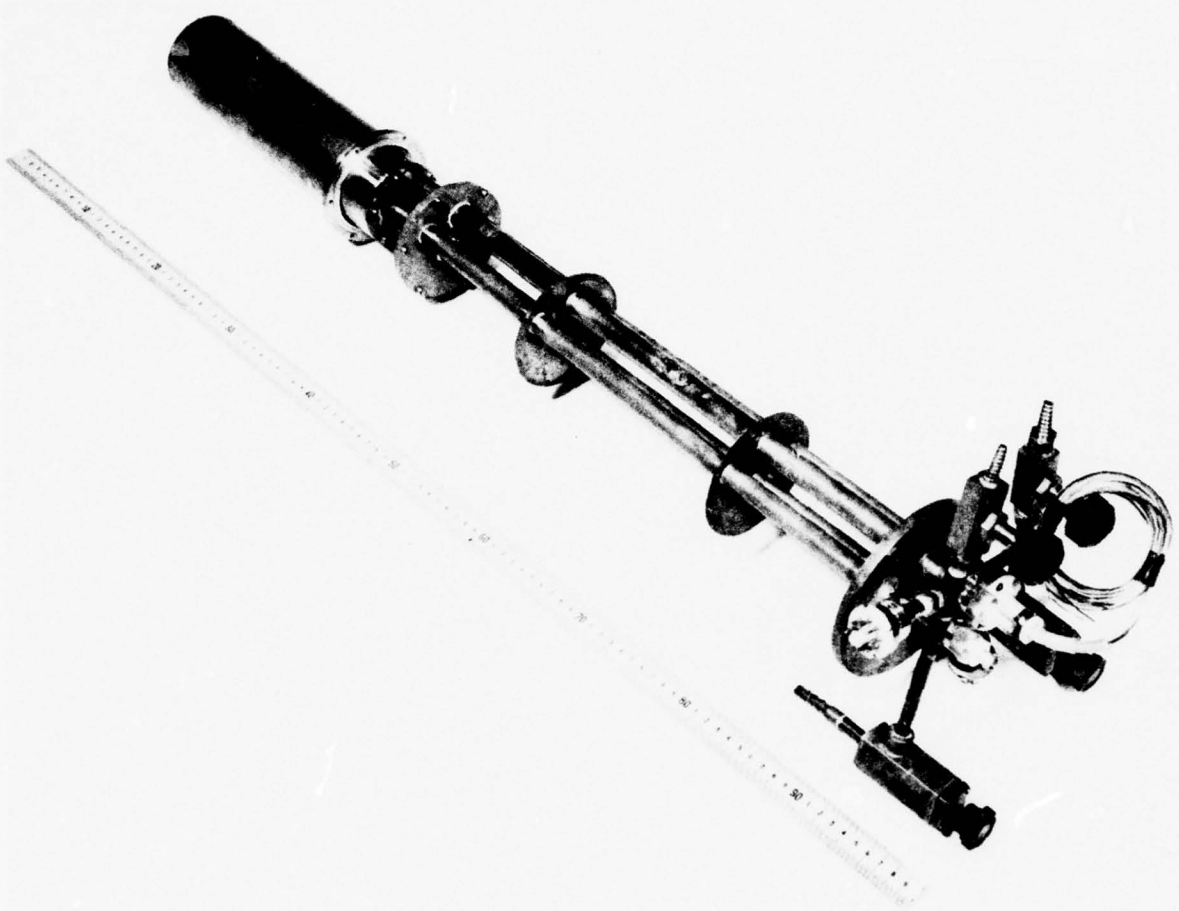

Figure IV.6. The Cryogenic Apparatus.

that the space between the cans can be evacuated. This provides an insulating jacket around the inner can. The cans are supported by three thin-walled cupro-nickel tubes. Two of the tubes have a smaller cupro-nickel tube centered inside the diameters of which were chosen to provide a 50Ω coaxial transmission line: one for rf input to the transducer and the other for the output from the detector. These tubes are also used as vacuum lines to the detector cavity and the outer can. The other tube houses the leads to the temperature sensors and to the heater, and also is used to supply a pressure to the inner can.

The gap spacing is controlled pneumatically as follows. The capacitive receiver is similar to that of the room temperature apparatus, except that the lapped ring against which the sample rests is undercut approximately .015 inch to make it a flexible diaphragm as shown in Figure IV.7. The space above the sample is evacuated (through the tube which is also the transmission line for the signal from the detector) and the rest of the sample.

The entire apparatus is placed inside a helium research dewar. After sealing the dewar and pumping on the coolant (either liquid nitrogen or liquid helium), temperature below the room-pressure boiling point of the coolant may be obtained.

The temperature around the sample is controlled by an electrical resistance heater which is connected to a standard commercial temperature controller.

The temperature measurements are made by sending a measured current from a constant current generator through the sensors (platinum or

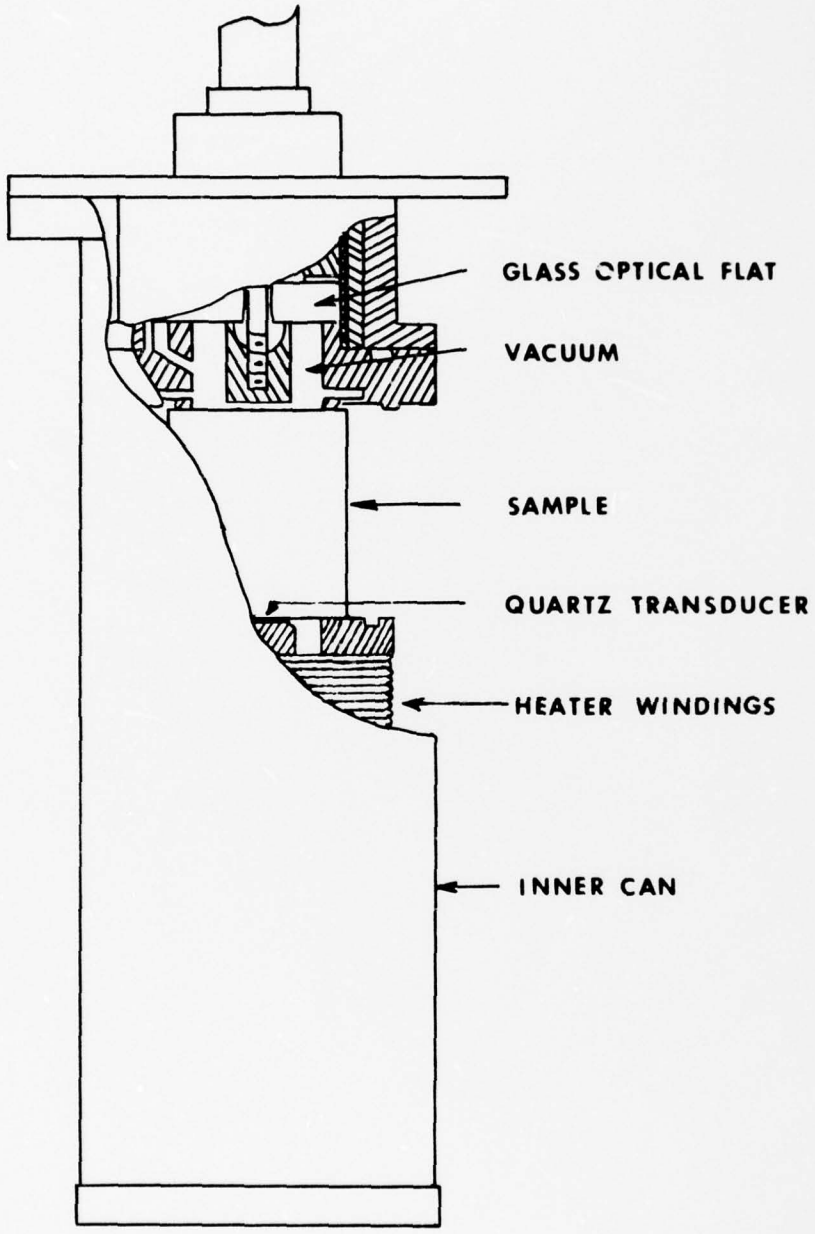

Figure IV.7. Cutaway View of Cryogenic Apparatus Showing the Variable Gap Capacitive Receiver.

germanium) mounted next to the sample and measuring the voltage across the sensors with a high input impedance (1000 MΩ) dc voltmeter. The resistance of the sensor is calculated and the temperature is determined from a sensor resistance versus temperature calibration curve furnished by the manufacturer.

Cryogenic Nonlinearity Measurements

The relative amplitude cryogenic measurements are made with the equipment arrangement shown in Figure IV.8. The signal paths are the same as with the room temperature apparatus except that no substitutional signal is introduced here.

The basis for the experimental procedure for making relative amplitude measurements may be seen from an examination of the expression for calculating the third-order elastic constant C_{111} (Eq. IV.1) $[C_{111} = -(\frac{8}{3}\frac{A_2}{A_1^2 k^2 a} + 1)3\, C_{11}]$. It is seen that if the fundamental wave amplitude A_1 is maintained constant as a function of temperature, then changes in C_{111} result from changes in C_{11} and the second harmonic amplitude A_2. Changes in C_{11} are determined from independent measurements.

To maintain A_1 constant, it is necessary only to maintain a constant 30 MHz amplifier output into the boxcar integrator by suitable changes in the rf drive voltage the transducer. This is done while maintaining a constant bias voltage across the capacitive receiver and keeping the receiver spacing (and hence capacitance) constant.

With A_1 held constant as a function of temperature, the relative measurements are made on the second harmonic amplitudes. Let the output of the 60 MHz amplifier be expressed as V_0. Let the amplitude of the

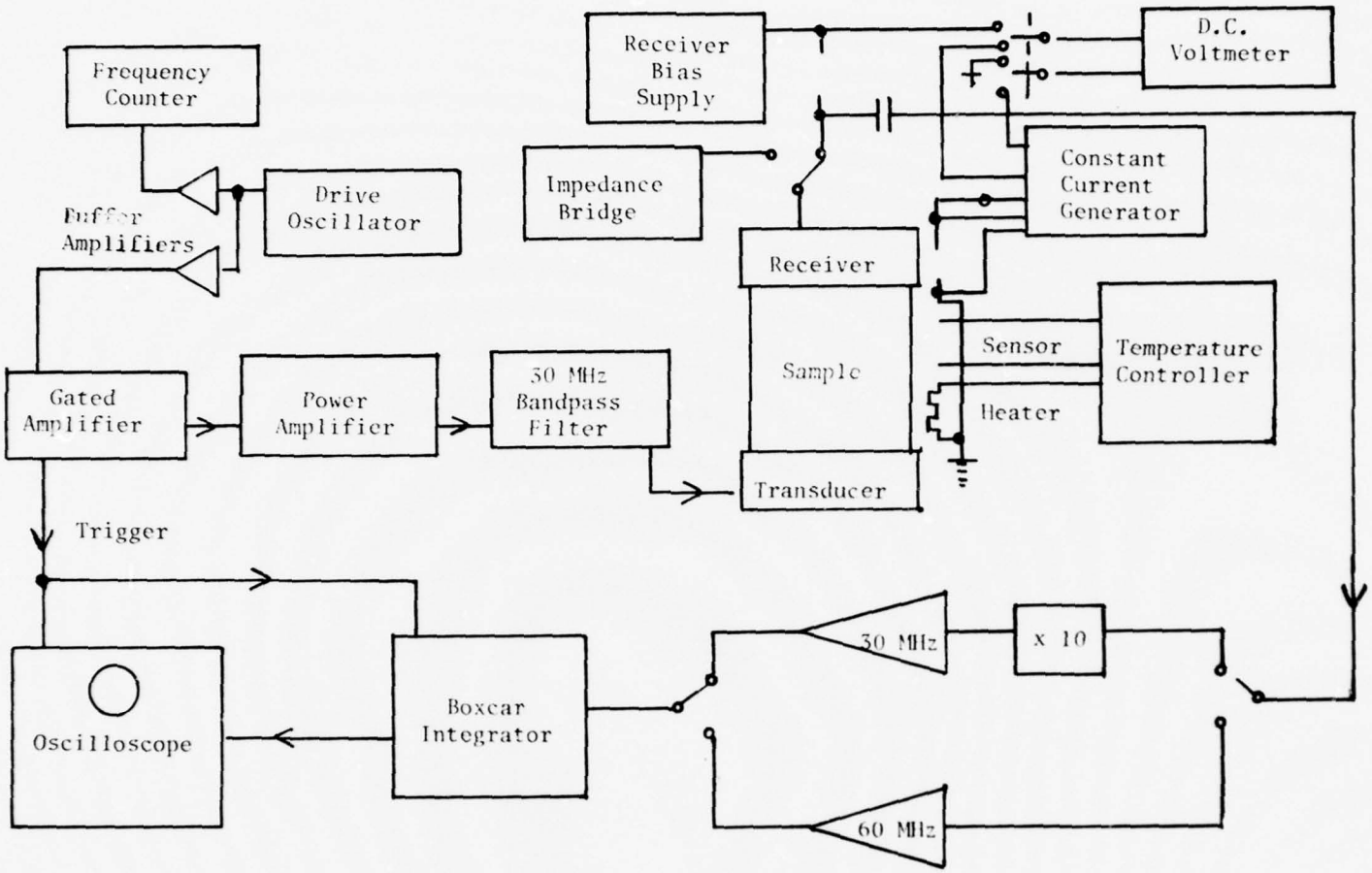

Figure IV.8. Block Diagram for the Cryogenic Nonlinearity Measurements.

second harmonic be A_2 and the capacitive receiver bias voltage be V_b. If the capacitance of the capacitive receiver is held constant as a function of temperature, then so is the gap spacing. Hence, we may write from Eq. (IV.2) that at some temperature T

$$V_0 = KA_2V_b \tag{IV.6}$$

where K is a constant. At the reference temperature T^R (room temperature), we may write the equation as

$$V_0{}^R = KA_2{}^RV_b{}^R \ . \tag{IV.7}$$

If the bias voltage V_b is altered at temperature T so that the output of the 60 MHz amplifier remains constant, i.e.,

$$V_0 = V_0{}^R \ , \tag{IV.8}$$

then

$$A_2 = A_2{}^R \frac{V_b{}^R}{V_b} \ . \tag{IV.9}$$

Hence, the relative amplitude measurements of the second harmonic may be obtained from measurements of the capacitive receiver bias voltage.

It can be shown from expression (IV.9) and Eq. (IV.1) that the ratio of C_{111} at temperature T to C_{111}^R at temperature T^R is (Peters, 1969)

$$\frac{C_{111}}{C_{111}^R} = \left(\frac{C_{11}}{C_{11}^R}\right)\left\{1 + \frac{\beta^R}{1+\beta^R}\left[\kappa^2 \frac{V_b{}^R}{V_b}\frac{C_{11}}{C_{11}^R} - 1\right]\right\} \tag{IV.10}$$

where

$$\beta^R = \frac{8}{3}\left[\frac{A_2}{A_1^2 k^2 a}\right]^R \qquad \text{(IV.11)}$$

$$\kappa = 1 + \alpha(T - T^R) \qquad \text{(IV.12)}$$

and α is the thermal expansion coefficient, which for fused silica is less than 10^{-6}, which is negligible in these experiments.

IV. VELOCITY MEASUREMENTS

The second-order elastic (SOE) constants C_{11} appear in both Eqs. (IV.1) and (IV.10). C_{11} is calculated from the expression

$$C_{11} = \rho V^2 \qquad \text{(IV.13)}$$

where ρ is the mass density of the material and V is the ultrasonic wave velocity in the appropriate direction. For fused silica the sonic velocity is independent of direction. The SOE constants were determined absolutely from room temperature velocity measurements by an ultrasonic pulse-echo technique. The tabulated data of A. Zarembowitch (1976) were used in the calculation of the relative cryogenic SOE constants.

The Capacitive Driver-Capacitive Receiver System

Until recently, it has been necessary to generate the ultrasonic pulses and to detect the resulting echoes in velocity measurements by applying bursts of rf to a piezoelectric transducer bonded to the specimen surface. Such an arrangement necessitates making a tedious correction in the velocity measurement due to ultrasonic wave phase shifts at the

specimen-bonded transducer interface. In some situations, the effect of this coupling between specimen and transducer leads to considerable error if neglected (McSkimin and Andreatch, 1962).

In order to eliminate the bond problem in compressional wave measurements, the air-gap capacitive-receiver used previously to measure amplitudes of ultrasonic waves (Gauster and Breazeale, 1966; Peters, Breazeale, and Paré, 1968) was modified to function as an air-gap capacitive driver as well (Cantrell and Breazeale, 1974). The air-gap capacitive driver-capacitive receiver combination allowed the sample ends to vibrate with free-free boundary conditions exactly. No bond corrections were necessary because there were no bonds.

More recently, a dielectric capacitive driver was developed to replace the air-gap driver (Cantrell and Breazeale, 1977). The new driver is capable of generating much larger longitudinal ultrasonic pulses than the previous one because one can apply larger voltages. Free-free boundary conditions still exist at the sample surfaces with this driver and the error in velocity measurements, without making any corrections, is comparable to the error in velocity measurements made with bonded transducers, after corrections for bond phase shifts.

The mechanical parts of the dielectric capacitive driver-capacitive-receiver system are the same as the room temperature apparatus (see Figure IV.2, page 35), except that the substitutional signal capabilities are not used and the quartz transducer is replaced with a piece of mica 0.625 inch in diameter and approximately 0.0002 inch thick. The mica is bonded to neither the sample nor the driver button.

A schematic of the dielectric capacitive driver is shown in Figure IV.9. The sample surface (outer electrode) is designated as (1) and the driver button (inner electrode) is designated as (5). Between the electrodes and the central mica dielectric (3), two air layers (2 and 4) are present because of slight irregularities of the contact surfaces.

A pulsed sinusoidally varying rf voltage, $V = V_0 \sin\omega t$, applied between the electrodes (1 and 5), produces sinusoidally varying electric fields E_1, E_2, and E_3. It has been demonstrated (Legros, Lewiner, and Biquard, 1972) that the generation of ultrasonic waves in this situation is due to the effect of electrodynamic forces acting directly on the *ultrasonic wave propagation medium.* Hence, if E_3 is the electric field near the surface of the sample, the force per unit area, p, at this surface is

$$p = \frac{1}{2} \varepsilon_o E_3^2 \qquad \text{(IV.14)}$$

where ε_o is the dielectric permittivity of air. Since

$$E_3 = E_{3o} \sin\omega t \qquad \text{(IV.15)}$$

then

$$p = \frac{1}{2} \varepsilon_o E_{3o}^2 \sin^2\omega t = \frac{1}{4} \varepsilon_o E_{3o}^2 \, (1 - \cos 2\omega t) \, . \qquad \text{(IV.16)}$$

For present purposes, it is adequate to ignore the constant term in Eq. (IV.16) and consider only the cos 2ωt term. One sees that the pressure on the sample surface is applied at <u>twice</u> the frequency of the

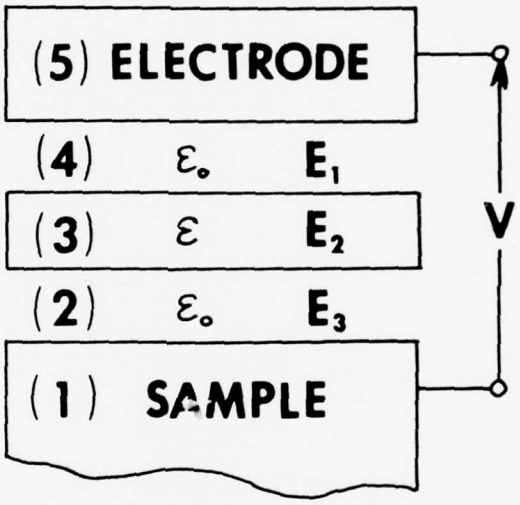

Figure IV.9. Schematic of the Dielectric Capacitive Driver.

rf voltage. Thus, the ultrasonic wave generated in the sample has twice the frequency of the applied rf voltage.

A Tuned Transmission Line Voltage Transformer

The capacitive transducer is driven with a pulsed rf signal. The frequency is varied around 15 MHz to produce successive resonances. To obtain the voltages necessary for adequate ultrasonic amplitudes, a specific length of transmission line was used to act as a tuned voltage transformer between the gated amplifier and the capacitive driver.

If S is the length of the transmission line, f the rf drive frequency, V_S the voltage across a purely reactive load of magnitude $|Z_L|$ (capacitive driver), V_0 the voltage out of the gated amplifier, and Z_0 the characteristic impedance of the transmission line, then for a lossless transmission line

$$V_S = V_0 \sin\phi \csc(\phi - \frac{\omega S}{c}) \qquad \text{(IV.17)}$$

where

$$\phi = - \tan^{-1} \frac{|Z_L|}{Z_0} \qquad \text{(IV.18)}$$

$$\omega = 2\pi f \qquad \text{(IV.19)}$$

and c is the velocity of propagation of electromagnetic waves in the transmission line. Thus, for the proper length S, $\frac{V_S}{V_0}$ becomes very large. But the impedance looking out of the gated amplifier into the transmission line behaves as

$$Z_{in} = -jZ_0 \tan(\phi - \frac{\omega S}{c}) \ . \qquad \text{(IV.20)}$$

Thus, for the condition that $\frac{V_S}{V_0}$ becomes large, Z_{in}, and consequently, V_0, become small. For this reason, the length of transmission line is chosen such that Z_{in} looks inductive for our operation frequency. A variable capacitor is then placed in parallel with Z_{in} to form a parallel resonant circuit. This arrangement increases the intensity of the generated ultrasonic signal by approximately 30 dB over that of the untuned transmission line.

The primary limitation on the generated ultrasonic wave amplitude is set by dielectric breakdown in the capacitive transducer. However, this limitation is not as serious as one might assume. As the spacing of the electrodes in air is decreased, the breakdown potential goes up almost exponentially (Cantrell and Breazeale, 1974). In the air-gap driver we were able to use fields as large as 200 $\frac{KV}{cm}$ without breakdown. With the mica dielectric driver, we have been able to use fields larger than 1000 $\frac{KV}{cm}$.

Method of Measurement

The velocity measurements were made with the equipment arrangement as shown in Figure IV.10. The gated double-pulse superposition method of Williams and Lamb (1958) was used. A pulsed ultrasonic wave is fed into the sample from the dielectric capacitive driver followed by another pulsed ultrasonic signal phase-locked but delayed in time with respect to the first. The delay is adjusted such that superposition of the desired echoes from the two pulse trains is achieved. The resulting signal is received at the other end of the sample by the air-gap capacitive receiver, passes through a 30 MHz bandpass amplifier and is displayed on an oscilloscope. Utilizing the fact that a continuous

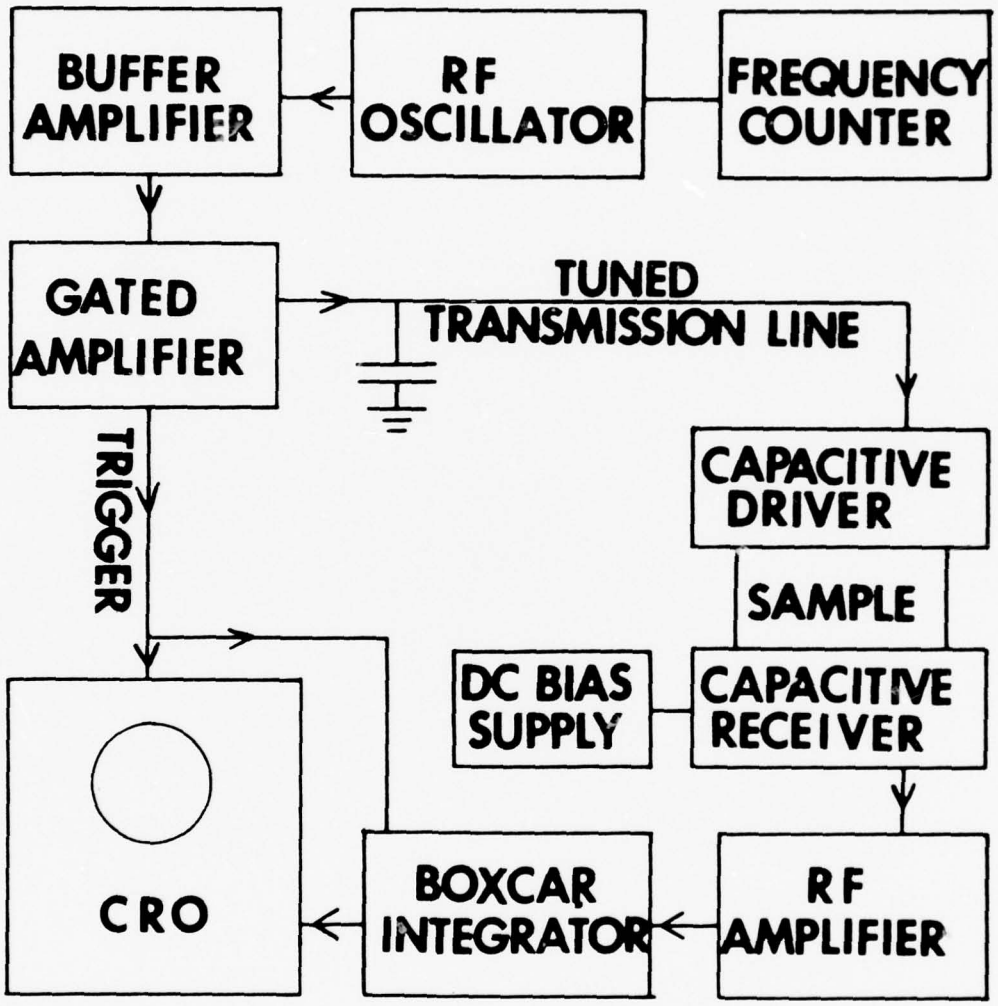

Figure IV.10. Block Diagram of Experimental Apparatus for Velocity Measurements.

change in ultrasonic frequency results in a succession of superimposed echo maxima and minima, the ultrasonic velocity is calculated from

$$v = 2m\ell \frac{\Delta f}{\Delta n} \qquad \text{(IV.21)}$$

where Δf is the change in ultrasonic frequency corresponding to Δn minima, ℓ is the sample length, and m is an integer (2 in these experiments) giving the relative position of the initial pulse train and the delayed pulse train. To enhance the sensitivity in detecting the superimposed echo minima, a boxcar integrator was incorporated into the system between the 30 MHz amplifier output and the oscilloscope.

V. SAMPLES AND SAMPLE PREPARATION

Samples

The fused silica samples used in this investigation were obtained from Amersil, Inc. of Hillside, New Jersey, and were manufactured under the commercial designation Suprasil. Suprasil represents a particular grade of fused silica which has been given a rating of Grade A, Type 458-677, according to military specification MIL-G-174.

Sample homogeneity is measured by the maximum variation in mass density of the material and in optics is most generally expressed as a change in refractive index (Δn) along an optical path. The Suprasil samples are designated as optical grades 1 and 2. The designation 1 implies a stated maximum variation of refractive index in all spatial directions, whereas the designation 2 implies a stated maximum refractive index variation in only one direction (perpendicular to the sample surfaces).

The designation W is used to distinguish the OH content of the samples. Those samples represented by the designation W contain approximately 5 ppm of OH content, whereas the unlettered samples have OH contents of approximately 1200 ppm.

Although all Suprasil samples contain less than 1 ppm of total metallic impurities, the Suprasil W samples contain approximately 260 ppm each of fluorine and chlorine impurities, whereas the unlettered samples contain about 130 ppm each of fluorine and chlorine.

All samples used in these experiments were approximately one inch in diameter. The length of each sample, the above mentioned impurity properties, and the measured ultrasonic velocities, at room temperature (27 °C), are tabulated in Table IV.1.

TABLE IV.1

SAMPLES USED IN THIS STUDY AND THEIR PROPERTIES

Sample	Impurity Content (ppm) OH	Fluorine	Chlorine	Sample Length (cm)	Longitudinal Ultrasonic Velocity ($x10^5$ cm/sec)
Suprasil—W1	5	260	260	1.2590±0.0003	5.9526±0.0016
Suprasil—W2	5	260	260	1.2587±0.0002	5.9533±0.0011
Suprasil 1	1200	130	130	1.2593±0.0002	5.9363±0.0012
Suprasil 2	1200	130	130	1.2586±0.0002	5.9363±0.0011

Since the fused silica samples are nonconductive, a conductive copper surface of the order of 1000 Å thick was evaporated onto the ends of the samples to form the ground potential electrodes for the transducer and detector.

Transducer Bonding for the Nonlinearity Measurements

The ultrasonic velocity measurements of the samples were made with the capacitive driver-capacitive receiver system and, hence, no transducers were bonded to the sample surfaces for these measurements. The use of a capacitive driver-capacitive receiver system for the low-temperature relative measurements of C_{111} would require extensive modification of the cryogenic apparatus to produce fundamental ultrasonic wave amplitudes large enough to generate measurable second harmonics. Further, the amplitude measurements of the first and second harmonics do not depend upon superposition of ultrasonic pulse-echo trains as did the velocity measurements. Hence, corrections for transducer bonds are not important for these measurements. For expediency, then, piezoelectric transducers were bonded to the sample surfaces for the nonlinearity measurements.

The transducers used in the nonlinearity measurements were X-cut quartz crystals bonded to the sample with the adhesive from a commercially available cellulose tape (manufactured by the Technical Tape Corporation, Carbondale, Illinois, under the designation 7510-551-9818, L590C, Type 1, Class A).

The adhesive was applied in the manner described by Yost (1972). A hole was cut in a plastic film having a diameter slightly larger than the diameter of the transducer. The hole was centered on the sample surface and a strip of tape was put over the hole. The tape stuck to the sample through the hole and air bubbles were rubbed out with a stick. Water was then applied to the tape backing and left until the water turned cloudy

(1 to 5 minutes). The water was then blotted away and the tape was gently lifted off. An amount of adhesive covering an area determined by the hole was left on the sample surface. The sample was left in a dessicator for twenty-four hours to remove excess moisture in the adhesive. The quartz transducer was then applied to the adhesive surface and bonded by rubbing the transducer firmly with the end of a teflon cylinder.

CHAPTER V

RESULTS AND DISCUSSION

I. ROOM TEMPERATURE NONLINEARITY MEASUREMENTS

The results of the absolute amplitude measurements at room temperature for all the fused silica samples are given in Table V.1.* A plot of A_2 versus A_1^2 for each sample is shown in Figures V.1, V.2, V.3, and V.4. The straight line in each of these figures is a least squares fit to the data points. It is seen that the data are fit very well with a straight line. The lines do not pass through the origin and the resulting A_2 intercept gives some measure of residual electronic noise (Bains, 1974) and is seen to be small for these measurements.

The slope of the line is (in the least squares sense) the best fit to the equation

$$A_2 = \frac{3}{8} \beta k^2 a A_1^2 \qquad (V.1)$$

and may be used to calculate the nonlinearity parameter β. However, a much more sensitive method to calculate β was developed by Yost (1972). In his method β is calculated from

---

*The measurements for the Suprasil 1 sample were repeated after noticing that the A_2/A_1^2 values of this sample were unusually high compared to the A_2/A_1^2 values of the other samples. The repeated data confirms the original measurements and eliminates the possibility that electronic instability introduced the high values of A_2/A_1^2.

TABLE V.1

AMPLITUDES OF ULTRASONIC WAVE COMPONENTS FOR FUSED SILICA SAMPLES MEASURED AT ROOM TEMPERATURE

Sample	Fundamental Amplitude A_1 (10^{-10} M)	Second Harmonic Amplitude A_2 (10^{-13} M)	$\frac{A_2}{A_1^2}$ (10^7 M^{-1})
Suprasil W1	1.006	1.793	1.772
	1.176	2.465	1.782
	1.308	3.101	1.812
	1.433	3.564	1.737
	1.534	4.154	1.765
	1.637	4.674	1.743
	1.731	5.160	1.723
	1.813	5.866	1.784
	1.864	5.923	1.703
	1.928	6.576	1.770
	1.996	6.932	1.739
	2.071	7.655	1.784
	2.147	8.142	1.767
	2.213	8.652	1.766
	2.278	9.187	1.771
	2.342	9.756	1.778
	2.385	10.292	1.809
	2.493	11.061	1.780
	2.622	12.343	1.796
	2.729	13.174	1.769
	2.858	14.361	1.758
	2.987	15.192	1.703
Suprasil W2	1.005	1.816	1.797
	1.179	2.448	1.761
	1.317	3.093	1.783
	1.429	3.702	1.812
	1.540	4.217	1.779
	1.635	4.815	1.801
	1.733	5.342	1.779
	1.820	5.857	1.769
	1.877	6.338	1.799
	2.032	7.380	1.788
	2.163	8.470	1.810
	2.301	9.524	1.799
	2.439	10.660	1.792
	2.556	11.515	1.763
	2.778	13.589	1.761

TABLE V.1 (continued)

Sample	Fundamental Amplitude A_1 (10^{-10} M)	Second Harmonic Amplitude A_2 (10^{-13} M)	$\frac{A_2}{A_1^2}$ (10^7 M^{-1})
Suprasil 1	0.948	1.698	1.887
Run 1	1.118	2.365	1.893
	1.251	2.983	1.905
	1.359	3.517	1.904
	1.471	4.002	1.849
	1.570	4.645	1.885
	1.653	5.226	1.912
	1.750	5.748	1.877
	1.807	6.197	1.898
	1.952	7.276	1.910
	2.088	8.307	1.906
	2.217	9.338	1.899
	2.327	19.320	1.906
	2.448	11.314	1.888
	2.667	13.460	1.892
	2.876	15.644	1.891
Suprasil 1	0.976	1.813	1.903
Run 2	1.274	3.078	1.896
	1.492	4.270	1.918
	1.682	5.356	1.893
	1.970	7.379	1.928
	2.246	9.555	1.894
Suprasil 2	1.009	1.767	1.735
	1.181	2.408	1.726
	1.312	3.048	1.771
	1.436	3.605	1.747
	1.544	4.151	1.742
	1.645	4.673	1.728
	1.737	5.289	1.753
	1.825	5.799	1.741
	1.887	6.321	1.775
	2.040	7.341	1.765
	2.190	8.539	1.780
	2.297	9.618	1.822
	2.448	10.543	1.760
	2.555	11.492	1.760
	2.770	13.520	1.762
	3.017	15.714	1.727
	3.242	18.085	1.721

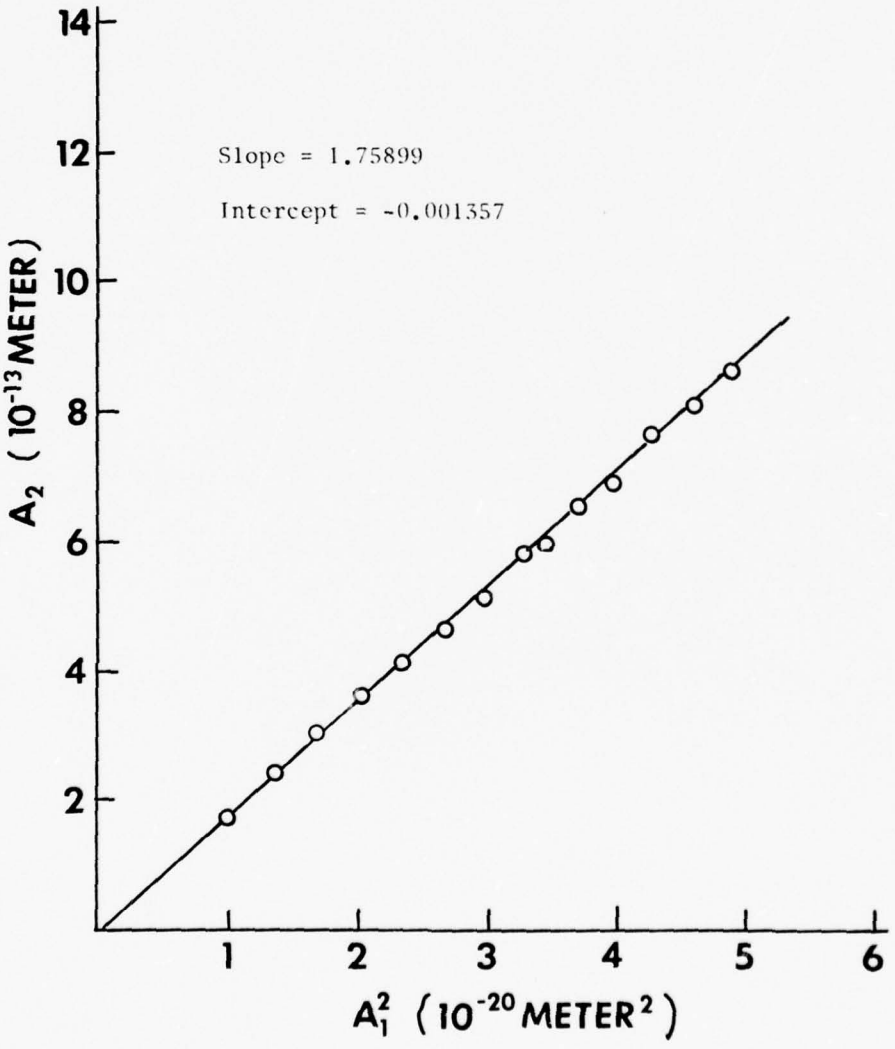

Figure V.1. A_2 versus A_1^2 for Suprasil W1.

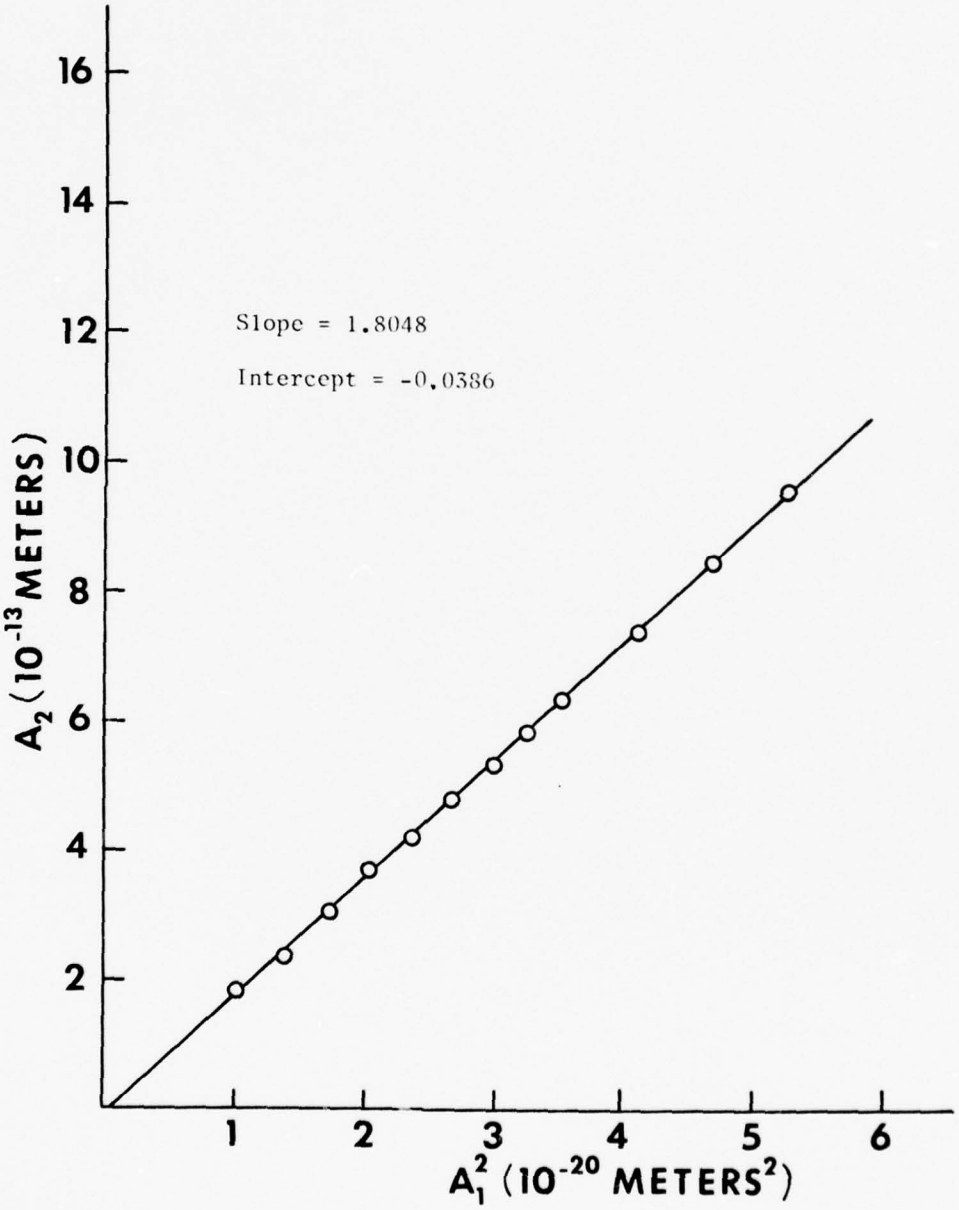

Figure V.2. A_2 versus A_1^2 for Suprasil W2.

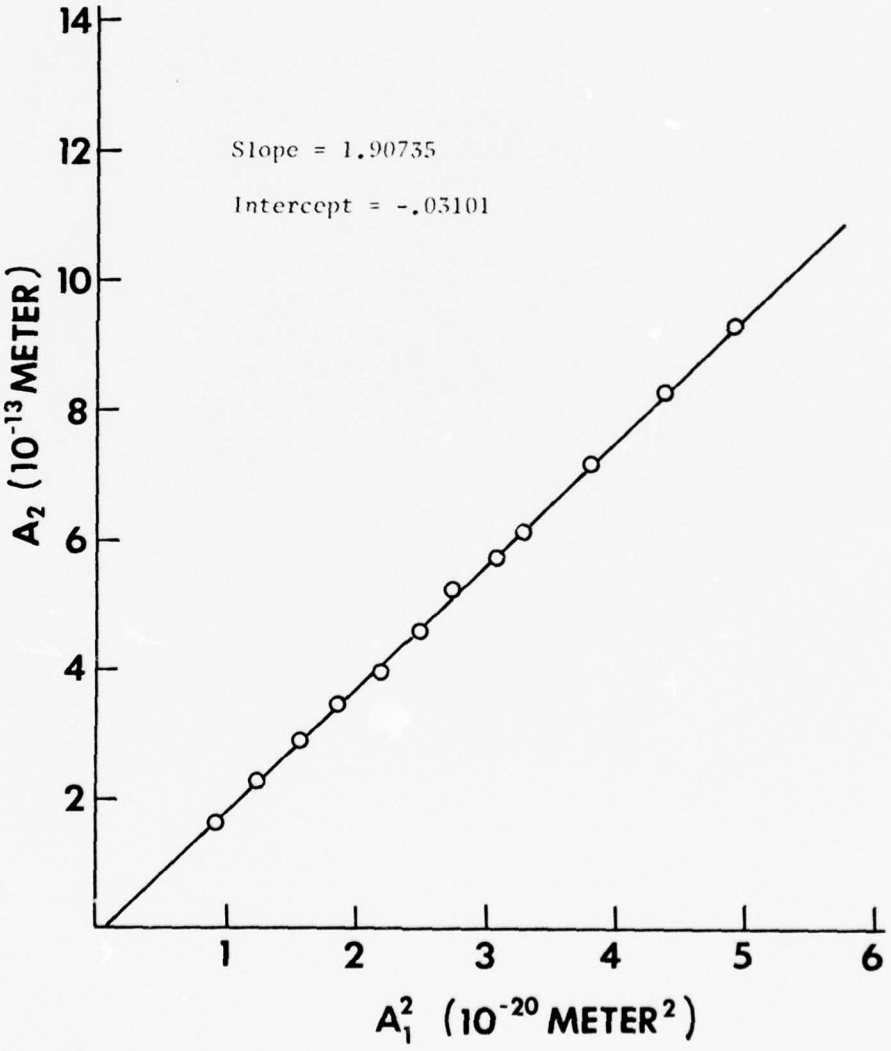

Figure V.3. A_2 versus A_1^2 for Suprasil 1.

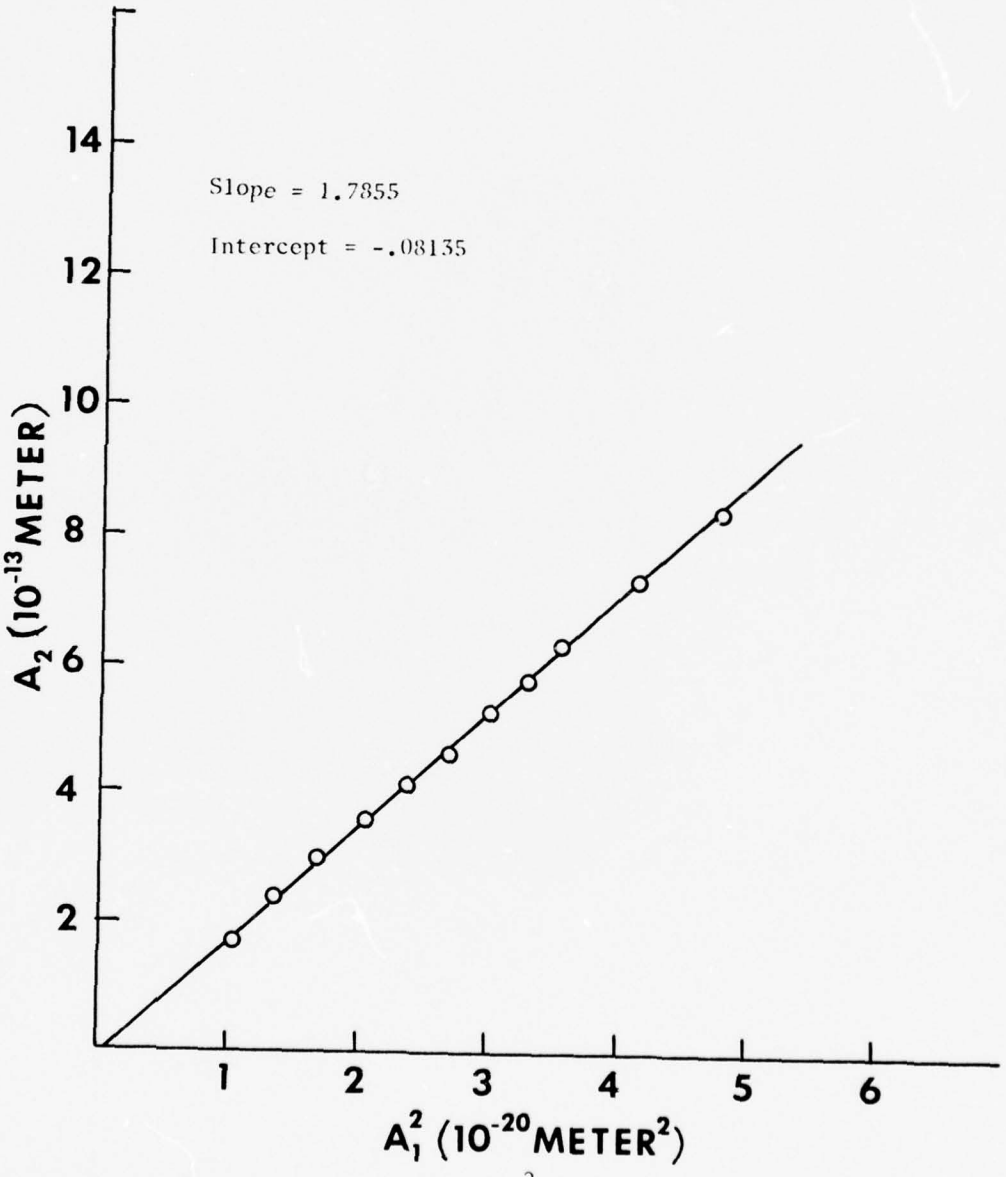

Figure V.4. A_2 versus A_1^2 for Suprasil 2.

$$\beta = \frac{8}{3}\frac{A_2}{A_1^2}\frac{1}{k^2 a} \qquad (V.2)$$

and is plotted as a function of A_1. This method allows measurements with good signal-to-noise ratios, and extrapolating the curve to zero value of amplitude A_1 gives a value of β which meets the theoretical assumption of infinitesimal amplitude waves (Thurston and Shapiro, 1967).

The β versus A_1 curves for each sample is given in Figures V.5, V.6, V.7, and V.8 and include the corrections for electronic noise obtained from the curves of Figures V.1, V.2, V.3, and V.4. The extrapolated β values are listed in Table V.2, along with calculated values of C_{11} and C_{111} at room temperature for each of the samples used in these experiments. The second-order elastic constants C_{11} are calculated from

$$C_{11} = \rho_o V^2 \qquad (V.3)$$

where ρ_o is the mass density of the samples and V the longitudinal ultrasonic velocity. The third-order elastic constants C_{111} are calculated from

$$C_{111} = -3C_{11}(\beta + 1) \; . \qquad (V.4)$$

II. TEMPERATURE DEPENDENCE OF β AND C_{111}

Table V.3 gives the measured relative values of β and C_{111} as a function of temperature. The temperature dependence of C_{11} was calculated from the data of A. Zarembowitch (1976) who measured C_{11} as a function of temperature for a sample of Puropsil fused silica. The temperature dependence of the samples used in this experiment are assumed to have the same relative temperature dependence as that of

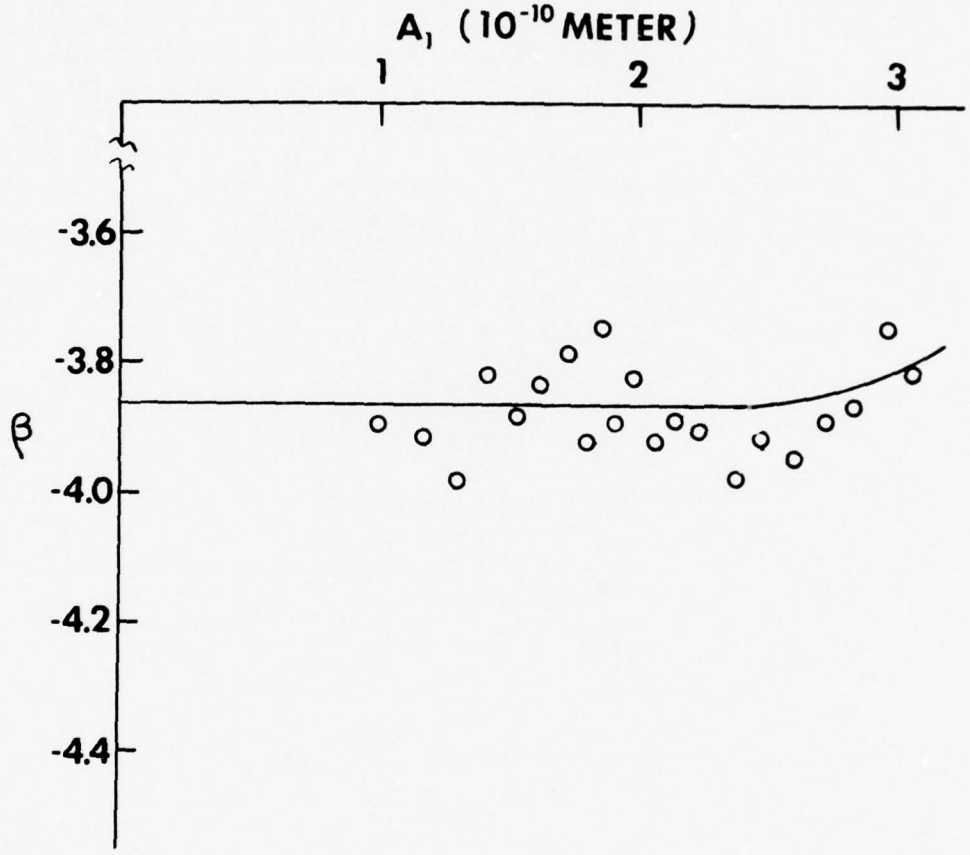

Figure V.5. Graph of β versus A_1 at Room Temperature for Suprasil WI.

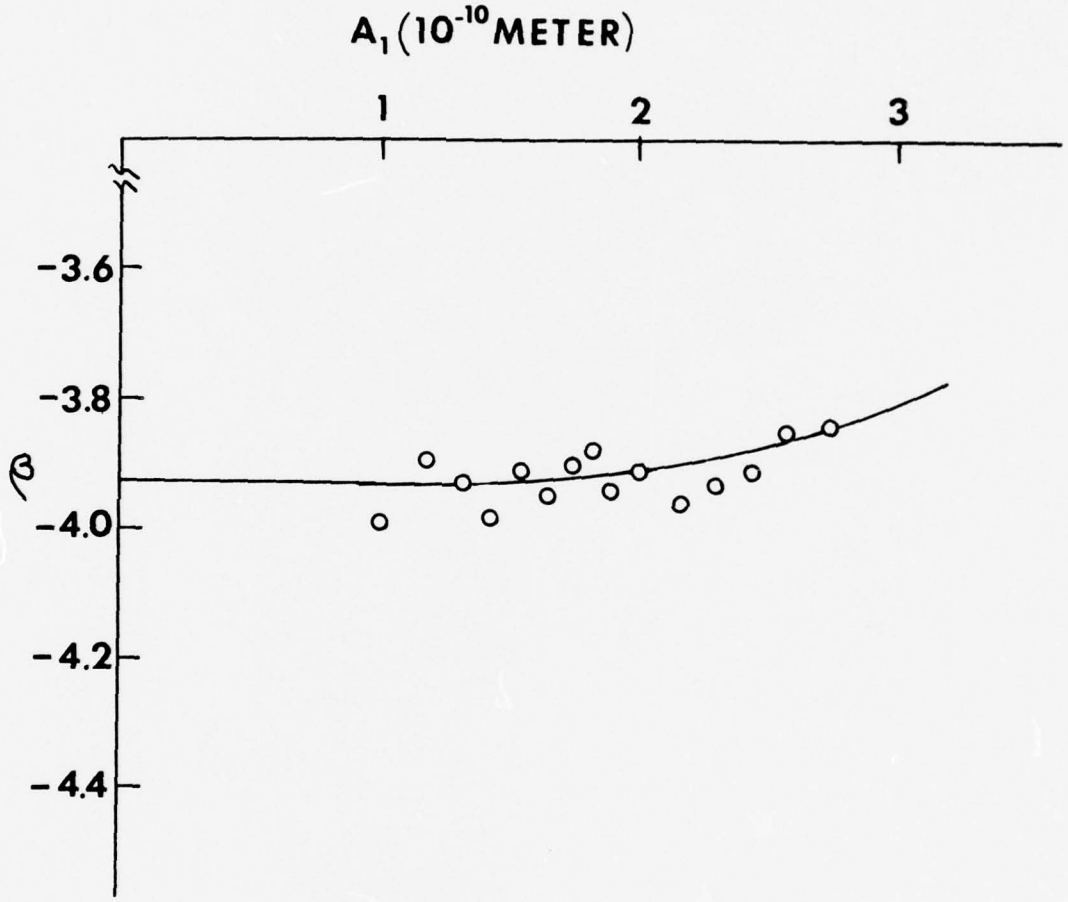

Figure 6. Graph of β versus A_1 at Room Temperature for Suprasil W2.

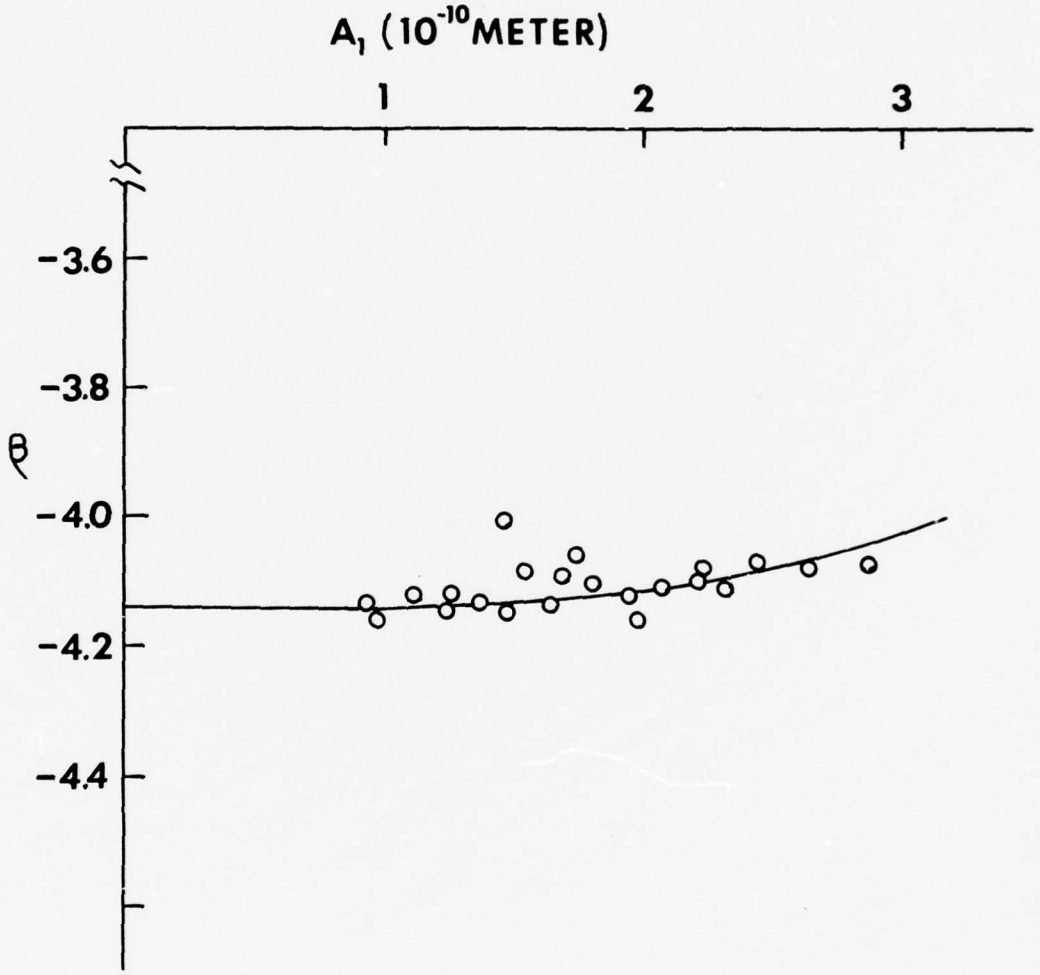

Figure V.7. Graph of β versus A_1 at Room Temperature for Suprasil 1.

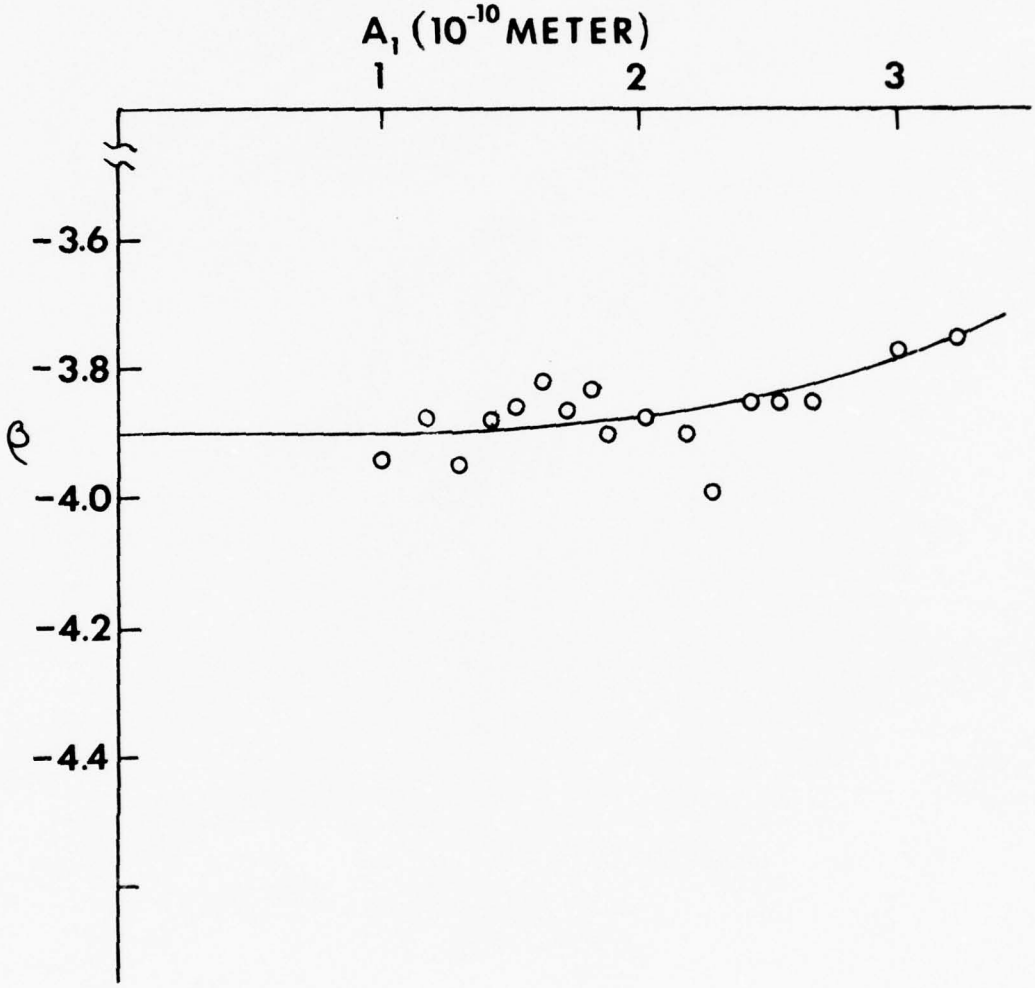

Figure V.8. Graph of β versus A_1 at Room Temperature for Suprasil 2.

TABLE V.2

MEASURED ROOM TEMPERATURE VALUES OF β, C_{11}, AND C_{111}[a]

Sample	β	C_{11} (10^{11} dynes/cm^2)	C_{111} (10^{12} dynes/cm^2)
Suprasil W1	-3.86 ± 0.071	7.8059 ± 0.0029	6.70 ± 0.124
Suprasil W2	-3.93 ± 0.034	7.8078 ± 0.0020	6.85 ± 0.058
Suprasil 1	-4.14 ± 0.041	7.7633 ± 0.0016	7.31 ± 0.073
Suprasil 2	-3.90 ± 0.039	7.7633 ± 0.0014	6.75 ± 0.067

[a]The errors listed are the calculated standard deviations (random errors).

TABLE V.3

MEASURED RELATIVE VALUES OF β AND C_{111} AS A FUNCTION OF TEMPERATURE

Sample	T (°K)	$\lvert\beta\rvert$	C_{111} (10^{12} dynes/cm^2)
Suprasil W1	2.9	3.765	6.276
	5.4	3.765	6.271
	6.5	3.763	6.262
	8.9	3.762	6.254
	18.8	3.768	6.256
	30	3.709	6.107
	42	3.746	6.178
	53	3.755	6.166
	65	3.810	6.307
	77	3.743	6.162
	88	3.584	5.814
	100	3.696	6.070
	112	3.744	6.187
	123	3.723	6.154
	136	3.732	6.184
	147	3.823	6.403
	159	3.760	6.275
	170	3.671	6.090
	181	3.815	6.432
	194	3.824	6.470
	205	3.842	6.522
	217	3.794	6.427
	233	3.812	6.490
	245	3.824	6.535
	259	3.825	6.556
	273	3.842	6.618
	282	3.855	6.663
	295	3.859	6.695
Suprasil W2	3.0	3.732	6.199
	5.1	3.803	6.353
	10.1	3.975	6.726
	18.8	3.697	6.093
	26.2	3.766	6.236
	36	3.846	6.405
	45	3.895	6.506
	77	3.811	6.310
	88	3.827	6.353
	100	3.785	6.265
	112	3.783	6.270
	123	3.681	6.053
	136	3.762	6.247
	147	3.763	6.262

TABLE V.3 (continued)

Sample	T (°K)	$\|\beta\|$	C_{111} (10^{12} dynes/cm^2)
	159	3.882	6.548
	170	4.026	6.891
	182	3.791	6.371
	195	3.764	6.328
	200	3.748	6.298
	209	3.872	6.590
	220	3.812	6.465
	289	3.863	6.688
	299	3.926	6.854
Suprasil 1	3.5	4.351	7.557
	8.8	4.387	7.623
	18.8	4.391	7.617
	30	4.285	7.356
	42	4.322	7.426
	53	4.280	7.321
	65	4.365	7.509
	77	4.357	7.494
	88	4.129	6.988
	100	4.368	7.535
	112	4.247	7.275
	122	4.380	7.589
	136	4.176	7.142
	147	4.386	7.634
	159	4.368	7.610
	172	4.285	7.443
	183	4.362	7.635
	194	4.383	7.701
	209	4.247	7.410
	221	4.115	7.123
	233	4.267	7.491
	245	4.183	7.317
	273	4.192	7.382
	282	4.245	7.523
	296	4.131	7.311
Suprasil 2	3.4	3.609	5.933
	8.8	3.629	5.965
	18.8	3.701	6.111
	30	3.698	6.091
	45	3.786	6.269
	77	3.712	6.099
	88	3.571	5.789
	101	3.653	5.982
	112	3.727	6.156

TABLE V.3 (continued)

Sample	T (°K)	$\|\beta\|$	C_{111} (10^{12} dynes/cm^2)
	124	3.815	6.367
	136	3.917	6.608
	147	3.914	6.615
	159	3.814	6.403
	172	3.829	6.454
	183	3.903	6.638
	194	3.876	6.593
	207	3.817	6.421
	226	3.829	6.474
	248	3.795	6.425
	264	3.850	6.578
	282	3.851	6.611
	299	3.899	6.752

Zarembowitch. Hence, accurate room temperature (reference temperature) measurements of C_{11} are all that is necessary for the calculation of the temperature dependence of the samples used in these experiments. These C_{11} values were then used in the calculations of C_{111} as a function of temperature for these samples.

Figures V.9, V.10, V.11, and V.12 show the temperature dependence of β and Figures V.13, V.14, V.15, and V.16 show the temperature dependence of C_{111} for each sample used in the present experiments.

III. ESTIMATE OF ERROR IN EVALUATION OF β AND C_{111}

The principal sources of systematic error in the room temperature measurements of β and C_{111} were the determination of the gap spacing in the capacitive receiver, the uncertainty in the amplitude of the calibration (substitutional signal) voltage, and the measurement of impedances in the room temperature apparatus. The R.F. voltmeter used in this study has a specified uncertainty of $\pm$ 2 percent full scale. The total systematic error in the temperature measurements of β and C_{111} are estimated to be within $\pm$ 12 percent. In addition, the random error (standard deviation) in the room temperature measurements are given in Table V.2 and are less than $\pm$ 2 percent.

The cryogenic measurements at a given temperature are estimated to be within $\pm$ 1 percent. This is based upon the measurements of Bains (1974) who determined this value after making several measurements of the ultrasonic wave amplitude over a period of time at one temperature.

The effect of changing temperatures on the quartz transducer bonds is difficult to assess and probably depends upon the amount of residual

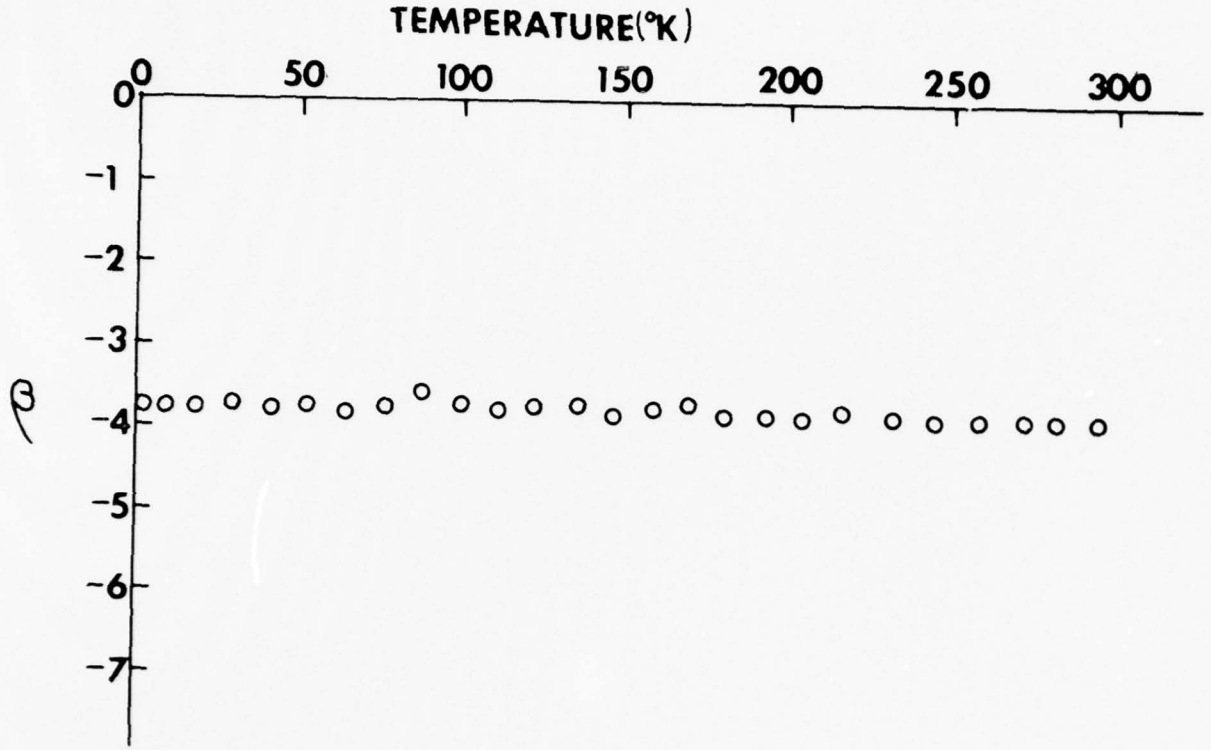

Figure V.9. β versus Temperature for Suprasil W1.

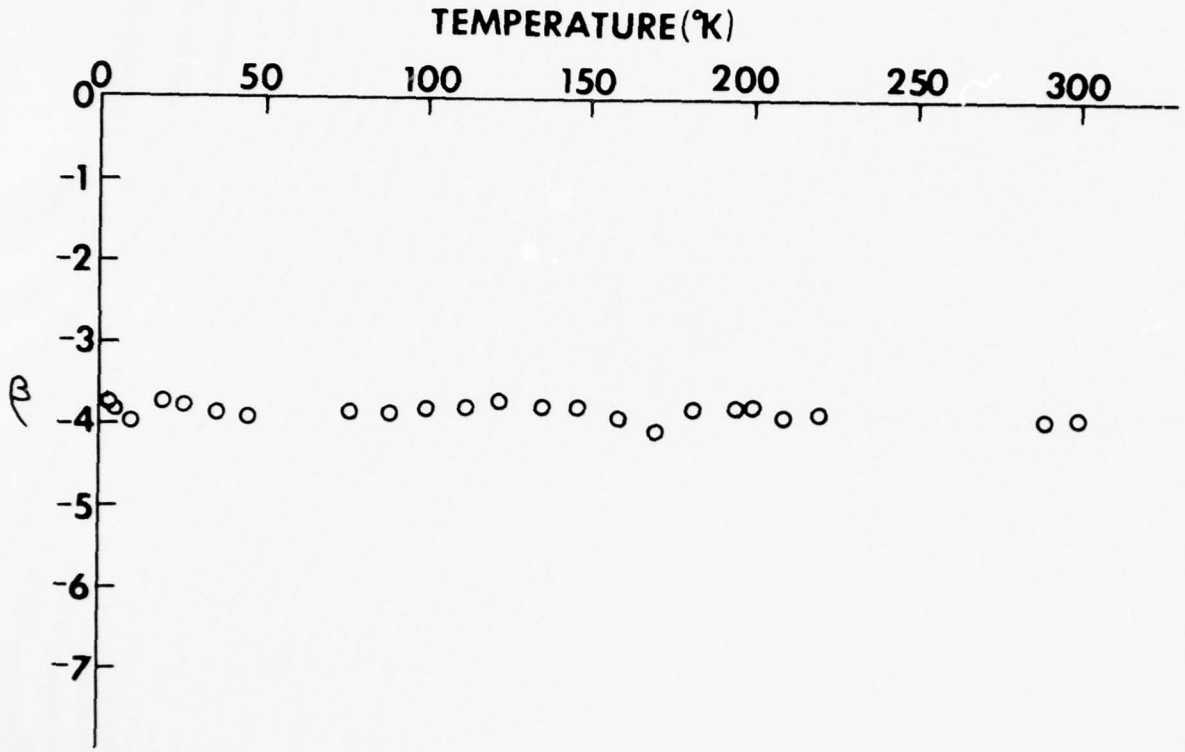

Figure V.10. β versus Temperature for Suprasil W2.

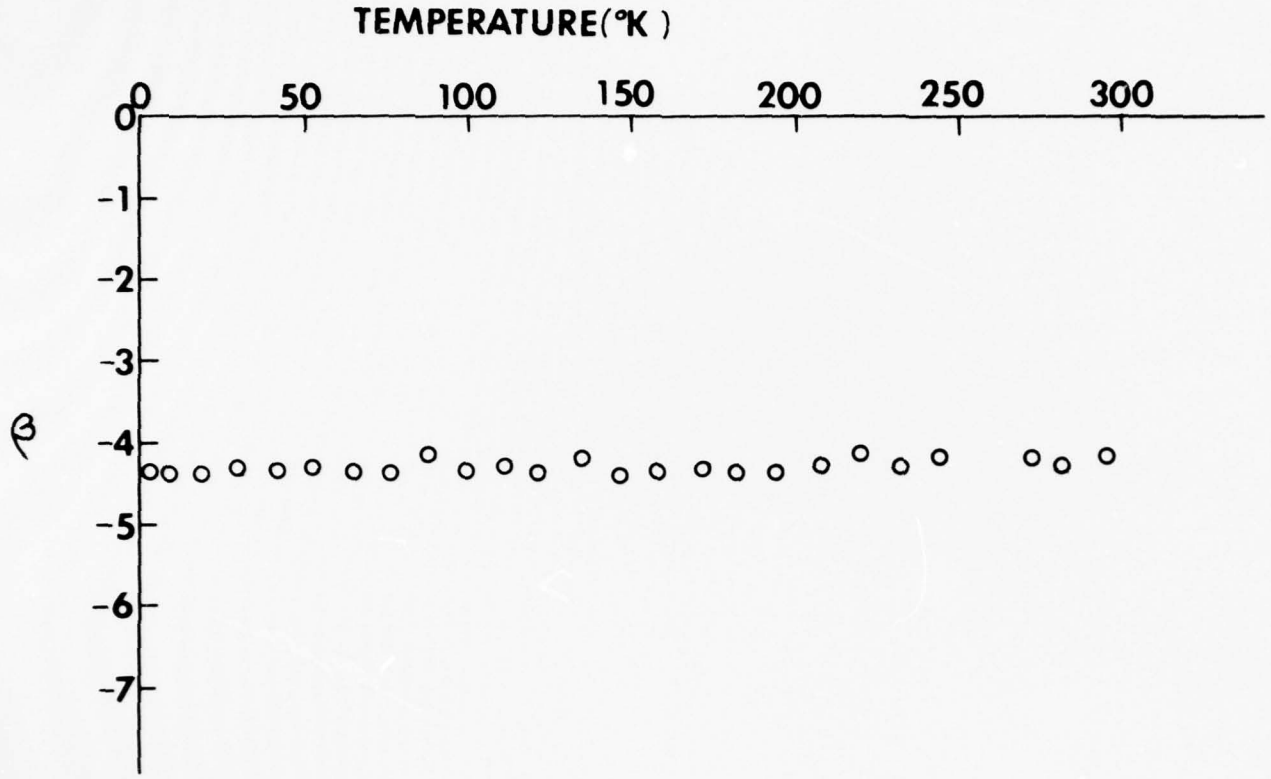

Figure V.11. β versus Temperature for Suprasil 1.

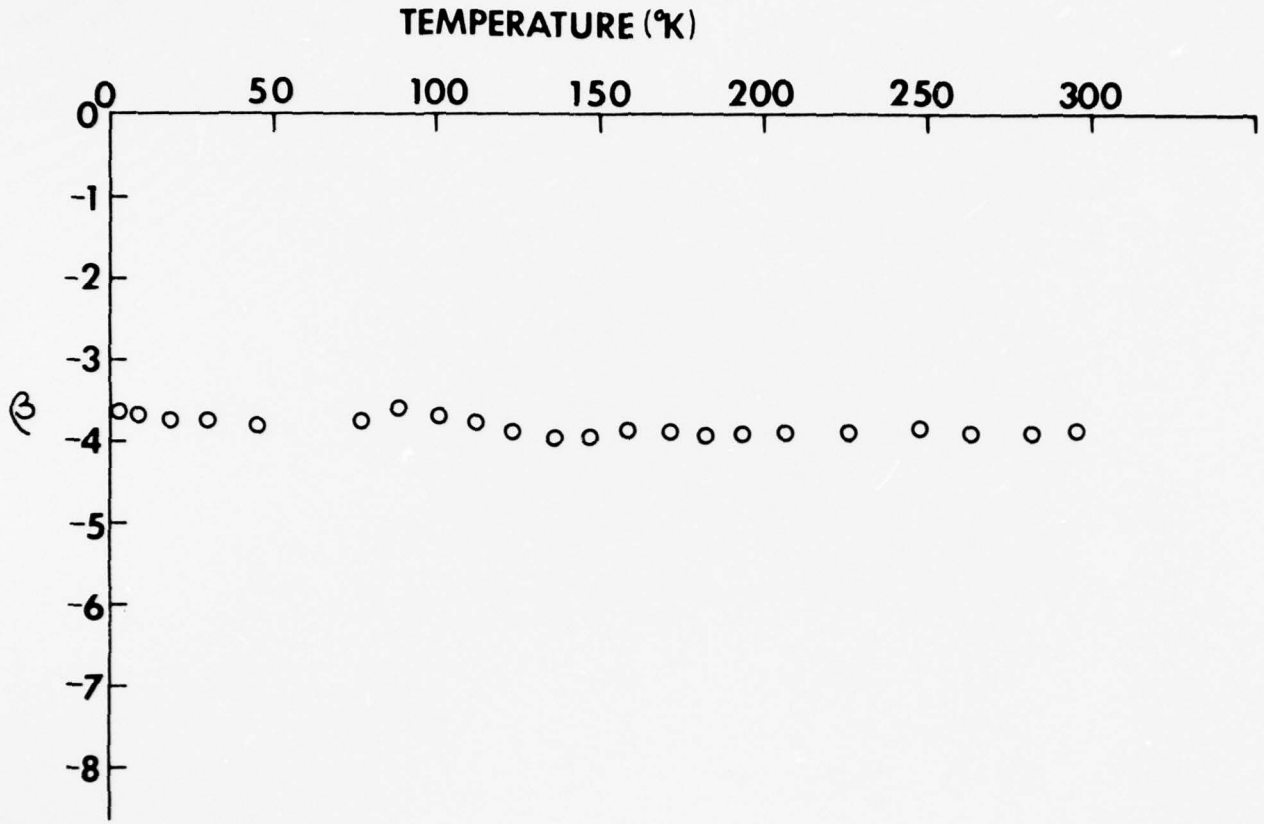

Figure V.12. β versus Temperature for Suprasil 2.

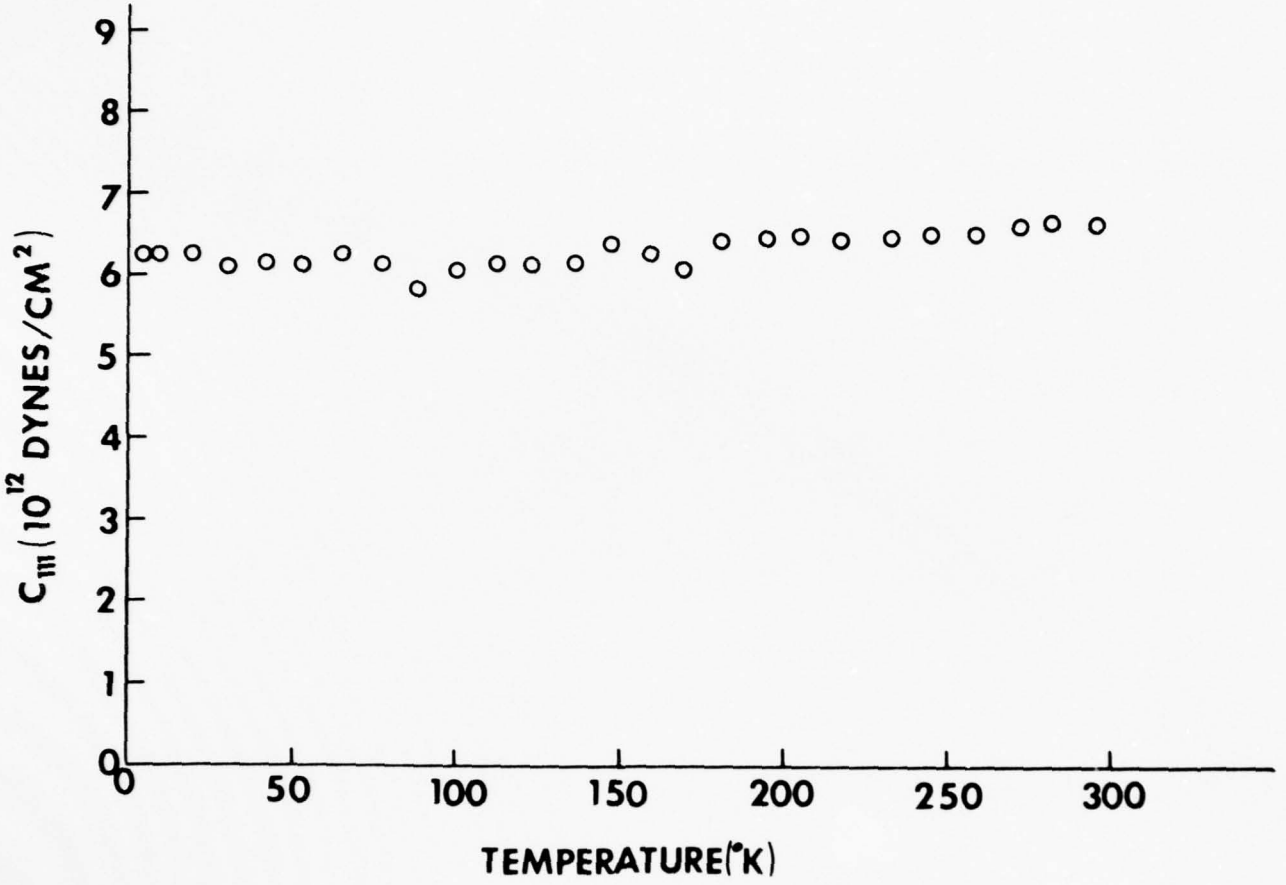

Figure V.13. Graph of C_{111} versus Temperature for Suprasil WI.

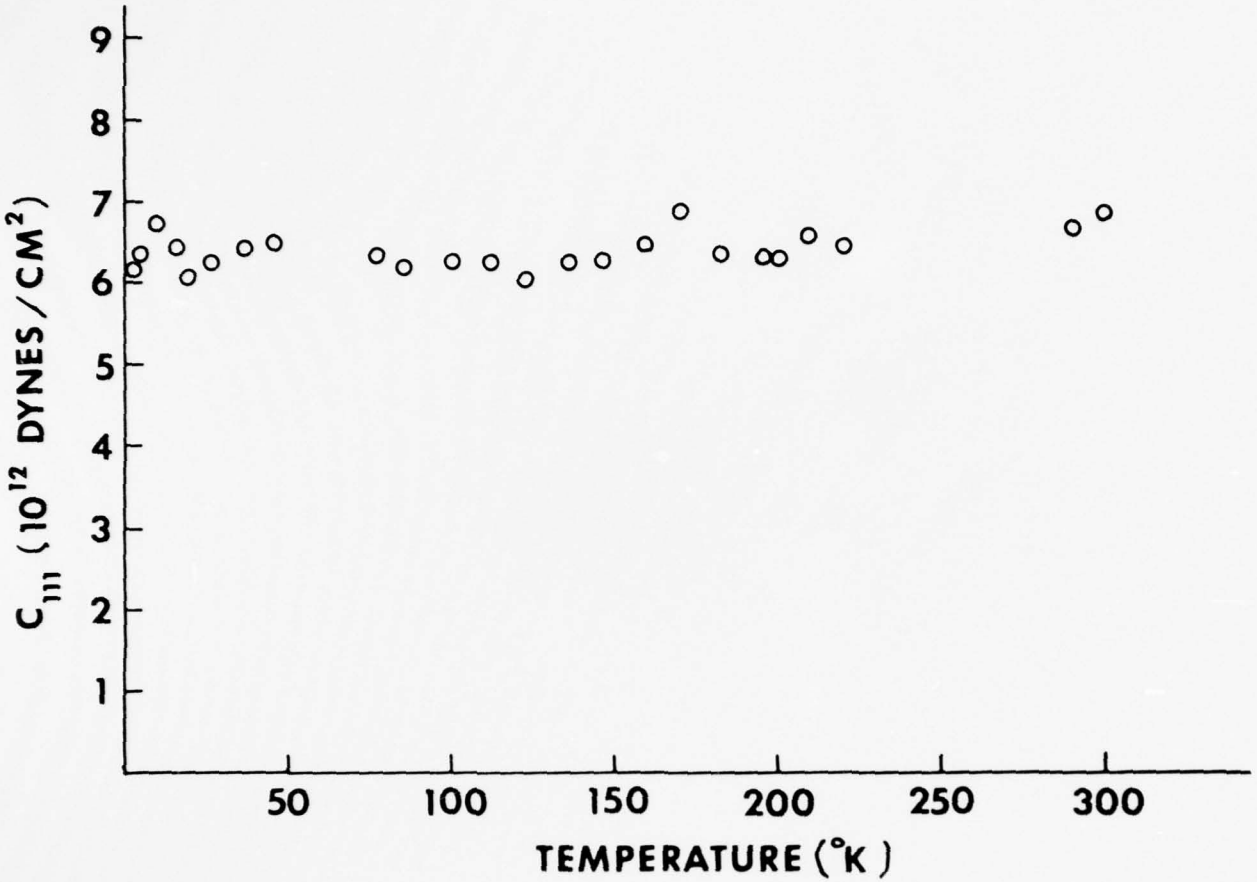

Figure V.14. Graph of C_{111} versus Temperature for Suprasil W2.

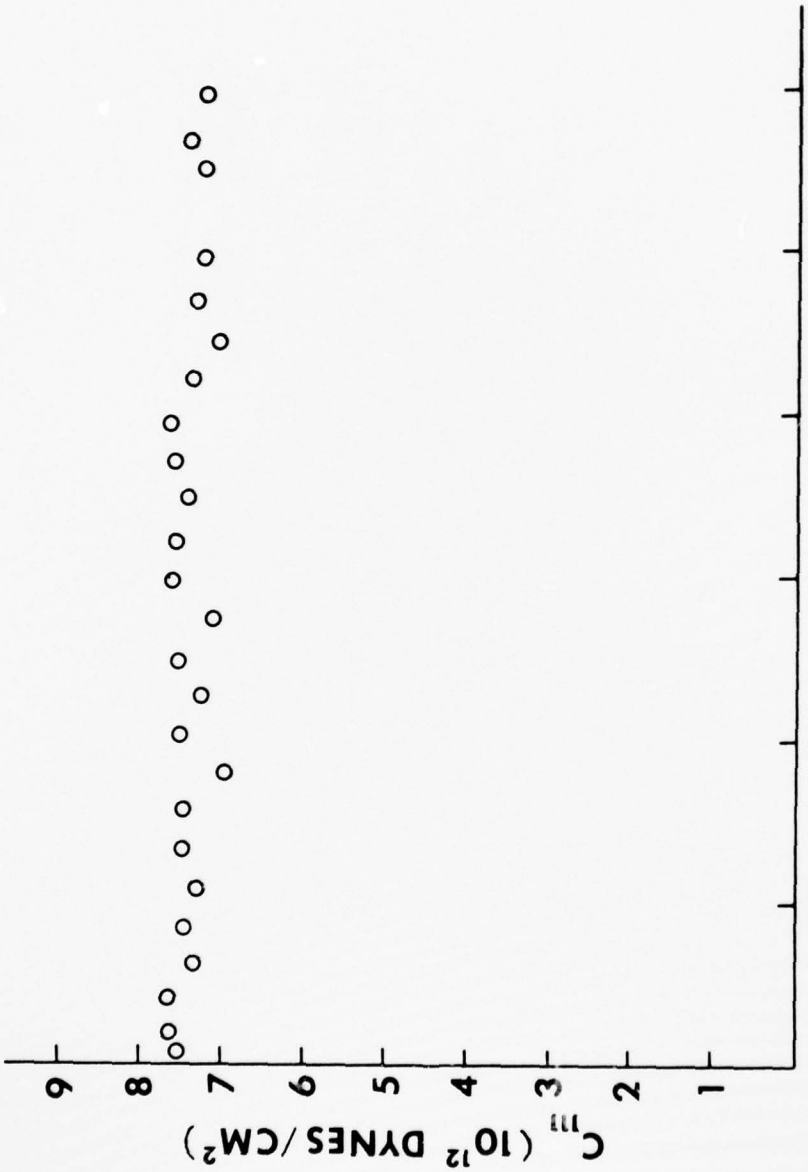

Figure V.15. Graph of C_{111} versus Temperature for Suprasil 1.

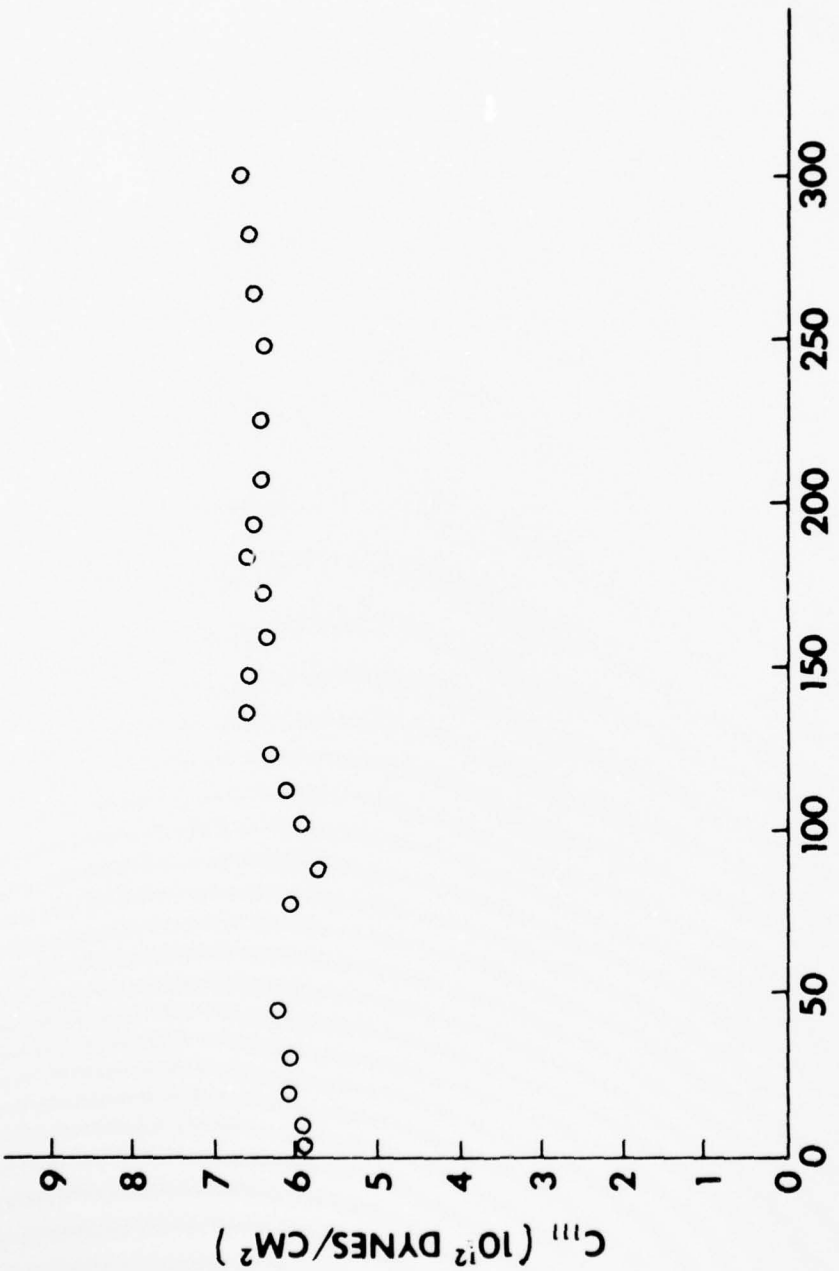

Figure V.16. Graph of C_{111} versus Temperature for Suprasil 2.

water content in the bonding material (cellulose tape glue). A reasonable estimate would be that the random error contributed by temperature changes in the transducer bonds is no more than ± 3 percent. This number was obtained from a comparison of measurements at a given temperature after cycling through a temperature range of approximately 120 degrees.

In summary, the total error in the room temperature measurements of the absolute ultrasonic wave amplitudes is estimated to be no greater than ± 14 percent. The total error in the relative cryogenic measurements is estimated to be no greater than ± 4 percent.

IV. THE STRUCTURE OF FUSED SILICA

Extensive x-ray diffraction studies of fused silica conducted primarily by Warren (1937) have confirmed the structural arrangement suggested by Zachariesen (1932). These studies reveal that the basic structure of fused silica is that of a silicon atom tetrahedrally surrounded by four oxygen atoms. The tetrahedra are then linked together through the Si-O-Si bonds in a random network arrangement. Breaks in the structure occur every 4th to 20th tetrahedron (Primak, 1975) and are often an impurity site. The average Si-O distance is about 1.6 Å and the average Si-Si distance is about 3.0 Å.

The Si-O bonding is neither covalent nor electrovalent but a combination of both (Simon, 1958). The electrovalent character of the Si-O bonds are responsible for rapid reforming of broken bonds but the covalent character results in a structure which is not readily

rearranged. The covalent character also leads to a normal Si-O-Si bond angle of approximately 140°.

V. DISCUSSION OF THE ROOM TEMPERATURE EXPERIMENTAL RESULTS

An examination of Table V.2, page 72, reveals that the second-order elastic constants of the fused silica samples with high OH content (Suprasil 1 and Suprasil 2) are lower than the samples with low OH content (Suprasil W1 and Suprasil W2). These results are consistent with those of Hetherington and Jack (1962) who noted also that an increase in OH content caused an increase in mass density fluctuations (inhomogeneity) as much as 3 parts in 10^3 in their experiments. Primak (1975) suggested that in similar measurements by Fraser (1968) in the ultrasonic range of frequencies the results reflect the effect of network cleavages induced by the OH impurities.

Table V.2 shows that β is negative for all the fused silica samples. This means that A_2 is also negative and [from Eq. (V.4)] that C_{111} is positive. Bains and Breazeale (1975) have shown, using a phase sensitive detector, that the harmonics of fused silica are generated out of phase with those generated by the same ultrasonic wave in copper. They conclude that the positive C_{111} of fused silica means that the solid becomes softer upon compression in contrast to copper which becomes stiffer upon compression.

According to Table V.2 Suprasil 1 has a substantially higher value of C_{111} than any of the other samples used in these experiments. It is tempting to infer that this is because of the high OH content of the

sample (1200 ppm compared to 5 ppm for Suprasil W1 and Suprasil W2), but Suprasil 2 also has high OH content (1200 ppm) and gives a value of C_{111} which lies between those of Suprasil W1 and Suprasil W2. A check for residual stresses in all the samples with crossed polaroid sheets revealed that all of the samples were stress free. Hence, the situation cannot be explained by residual stresses in a particular sample. A possible explanation may be that the Suprasil 1 sample is strongly homogeneous in all directions whereas the Suprasil 2 sample is strongly homogeneous only in the direction perpendicular to the sample faces (see Chapter IV, page 56). This means that mass density variations may exist across the face of the ultrasonic beam large enough to scatter large numbers of phonons. Since the amount of phonon scattering would be frequency dependent, fundamental and second harmonic phonons would be scattered in different amounts and could be such as to cause a decrease in the value of C_{111} for Suprasil 2 to that in Table V.2, page 72. If this is the case then from Table V.2 the values of C_{111} for the low OH content samples are lower than the C_{111} values for the high OH content samples. This is in contrast to the C_{11} values for the low OH content samples being higher than the high OH content samples. Thus, the network cleavages introduced by the OH impurities which may be the cause of lower C_{11} values may also be the cause of an increase in the C_{111} values.

VI. DISCUSSION OF TEMPERATURE DEPENDENT RESULTS FOR C_{111}

Figures V.13-V.16, pages 81-84, show a significant amount of scatter in the data points of C_{111} as a function of temperature.

AD-A035 376 TENNESSEE UNIV KNOXVILLE ULTRASONICS LAB F/G 20/1
AN ULTRASONIC INVESTIGATION OF THE NONLINEARITY OF FUSED SILICA--ETC(U)
JAN 77 J H CANTRELL N00014-71-A-0121-0001
UNCLASSIFIED TR-14 NL

2 OF 2
AD-A
035 376

END
DATE
FILMED
3-17-77
NTIS

Considering that the estimate of random error due to temperature changes in the transducer bonds was ± 3 percent and that the standard error was no more than ± 1 percent, the considerable amount of scatter would seem to indicate structural changes in the samples as a function of temperature. This is consistent with the suggestions of Primak (1975) who asserts that variations do occur in the structure of fused silica as the temperature is changed. This is in large part due to the asymmetrical nature of the void surrounding the oxygen atom which is a reflection of the random nature of the tetrahedral network. As the temperature is lowered evidence exists (Primak, 1975) that the Si-O-Si bond angle changes due to the asymmetrical vibrations of the oxygen atoms. Thus, the tetrahedral network of fused silica below the quenching temperature (the temperature at which the melt turns into a solid) is in a state of stress. The resulting states of strain are more accentuated for the weak impurity bonds and this makes them more efficient electron traps than the strong Si-O bonds. This means that the effect of temperature changes is to cause variations especially in anharmonic dependent effects since it is these effects that are most sensitive to variations in structural symmetry and strain perturbations introduced by impurity sites.

Although the systematic and random errors in the cryogenic measurements are too large to attach a great amount of significance to individual data points, trends in the C_{111} versus temperature data are apparent. The C_{111} values of Suprasil W1, Suprasil W2, and Suprasil 2 all show a general decrease of C_{111} with decreasing temperature. The C_{111} value of Suprasil 1 on the other hand certainly does not generally

decrease with decreasing temperature and may even exhibit a slight increase with decreasing temperature. As with the room temperature measurements, Suprasil 1 (with high OH content) seems to be an anomaly. Again, however, Suprasil 2 (also with high OH content) seems to show the general (maybe even more pronounced) C_{111} versus temperature behavior as Suprasil WI and Suprasil 2 (both with low OH content). Following the explanation given for the room temperature measurements, it is conceivable that the lack of strong homogeneity in the Suprasil 2 sample in all spatial directions gives rise to large density fluctuations across the face of the ultrasonic beam. The change of temperature may possibly exaggerate these density fluctuations thereby giving rise to the observed temperature dependence of C_{111} for Suprasil 2. The pronounced decrease of the C_{111} value of Suprasil 2 (Fig.V.16, page 84) with decreasing temperature in the range 147 °K to 88 °K indicates that a strong structural change (and consequent density changes) may have taken place.

VII. DISCUSSION OF THE TEMPERATURE DEPENDENT RESULTS FOR β AND ITS IMPLICATIONS FOR THE CALCULATION OF GRÜNEISEN'S GAMMA

The plots of β versus temperature (Figures V.9-V.12, pages 77-80) indicate that β is a much weaker function of temperature for all the samples used in these experiments than is C_{111}. Since the $\gamma_{11}(P_\ell,\hat{N})$ component of the strain generalized Grüneisen parameter for fused silica is directly proportional to β it is also weakly dependent upon temperature for these samples. This implies that any significant temperature variation in the volume generalized Grüneisen parameters for fused silica

[Eq. (III.13)] must come from significant variations in the elastic constants other than C_{11} and C_{111}.

It was mentioned previously that the Grüneisen parameter γ depends on temperature directly through the modal specific heats and indirectly through the combination of elastic constants in terms of which the volume generalized Grüneisen parameters may be expressed [Eqs. (III.22, III.43)]. Figure V.17 shows the experimentally determined Grüneisen parameter γ as a function of temperature as measured by White (1964) for fused silica (Spectrosil). It is seen that γ becomes negative between .2 and .3 of the Debye temperature (495 °K for Spectrosil) and continues to become more negative with decreasing temperature. As seen from Figure V.17 this is in contrast to germanium for which γ levels off as the temperature approaches zero and to quartz which maintains a positive Grüneisen parameter as a function of temperature.

It is apparent from Eq. (III.22) that in order to obtain a negative value of the Grüneisen parameter at some temperature at least one of the volume generalized Grüneisen parameters must be negative at that temperature since the modal heat capacities $C(p,\hat{N})$ are always positive. Barron (1957) and Blackman (1958) have suggested theoretical models which for some volume generalized Grüneisen parameters associated with certain transverse vibrational modes of that model do become negative. These transverse modes necessarily involve elastic constants other than C_{11} and C_{111}. White and Birch (1965) suggested that the transverse vibrations of fused silica are associated with the oxygen atoms of the tetrahedral network.

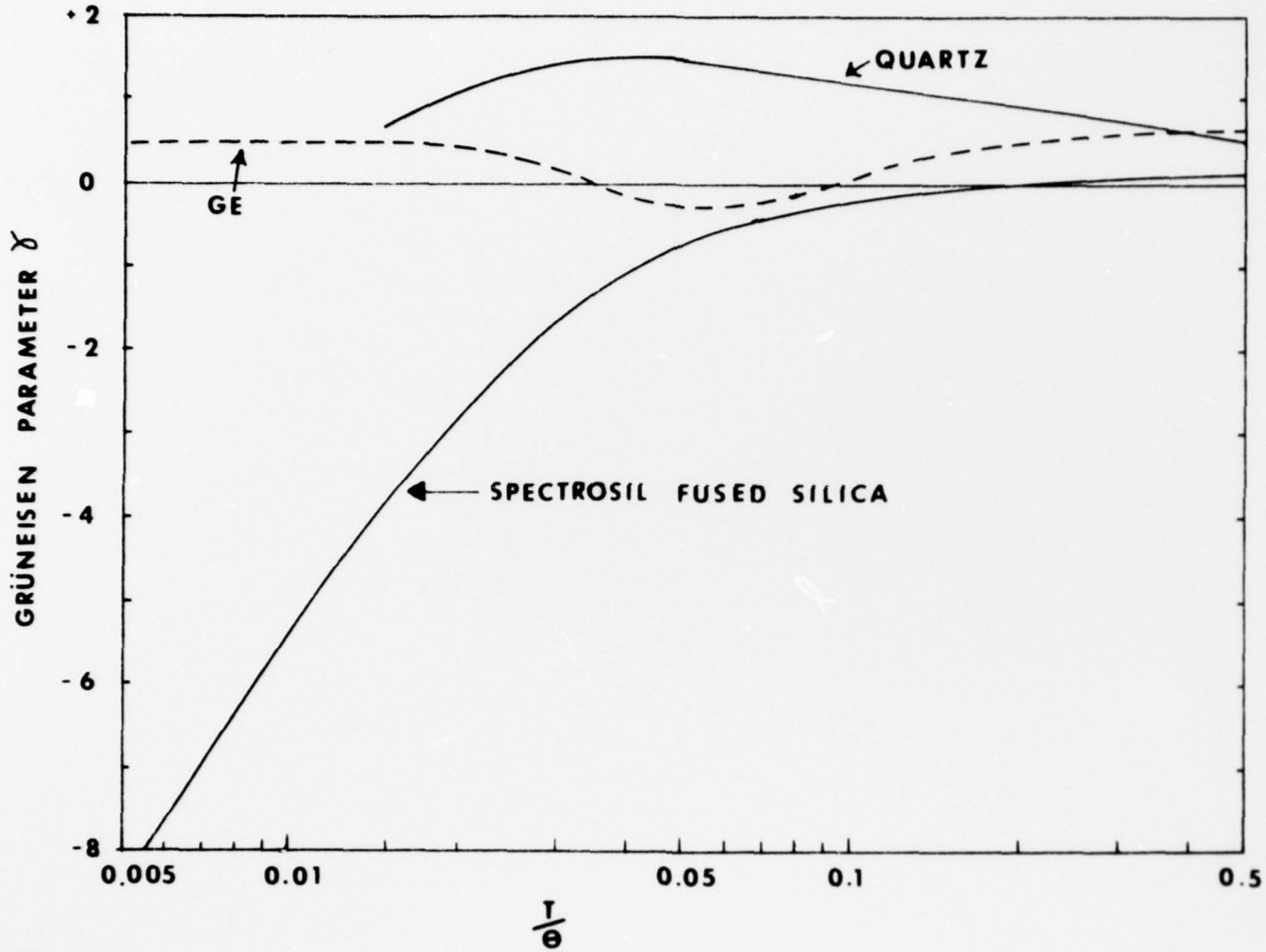

Figure V.17. Graph of Grüneisen Parameter versus Reduced Temperature for Quartz, Germanium, and Fused Silica (G. K. White, 1964).

According to Eq. (III.22) the calculation of the Grüneisen parameter depends strongly on the modal heat capacities $C(p,\hat{N})$ which serve as "weighting" functions of the $\gamma(p,\hat{N})$. Further, the denominator of the expression is the Debye heat capacity. Experimentally determined measurements of the heat capacities for fused silica at low temperature reveal that the experimental values are larger than the calculated Debye heat capacity by a factor of 5 at certain temperatures. Flubacher, Leadbetter, Morrison, and Stoicheff (1959) suggested from Raman and Brillouin spectra experiments that the "excess" heat capacity of fused silica is contributed by optical modes of very low frequencies and unknown origin. They showed that the addition of three Einstein heat capacity terms of low optical mode frequencies to the calculated Debye heat capacity gives good agreement with experiment.

Clark and Strakna (1962) suggested two equilibrium positions for the oxygen atoms (double potential well) to explain the "excess" heat capacity but their suggestion fit the experimental data above 2 °K less well than the optical mode model of Flubacher et al. (Leadbetter and Morrison, 1963). However, Arnold, Hunklinger, Stein, and Dransfeld (1974) have recently applied the double potential well model to ultrasonic attenuation at gigahertz frequencies in fused silica below 2 °K and have found good qualitative agreement with experiment.

In conclusion, the present experimental determination of β and C_{111} as a function of temperature allows an important inference to be made regarding the temperature dependence of the Grüneisen parameter for fused silica. If the quasiharmonic Debye model of a solid is assumed to hold for fused silica, then the relatively weak temperature

dependence of β and C_{111} indicates that elastic constants other than C_{11} and C_{111} must dominate the strong temperature dependence of the experimentally determined Grüneisen parameter for fused silica at low temperatures. This is consistent with the arguments presented by Barron (1957), Blackman (1958), White and Birch (1965), and Primak (1975) that the transverse vibrations of the oxygen atoms in the tetrahedral network of fused silica give rise to negative values of the Grüneisen parameter at low temperatures. The elastic constants associated with these transverse modes would be of the type C_{12}, C_{44}, C_{144}, C_{456} for solids in general. For fused silica there are only two independent second-order elastic constants (C_{11} and C_{44}) and three independent third-order elastic constants (C_{111}, C_{144} and C_{456}). Therefore, only C_{44}, C_{144}, and C_{456} would dominate in the transverse modes for fused silica.

VIII. SUGGESTIONS FOR FURTHER WORK

The results of this study have raised a number of questions to be investigated.

1. The temperature dependence of the Grüneisen parameter β in fused silica cannot be fully understood until the elastic constants other than C_{11} and C_{111} are measured as a function of temperature. The ultrasonic beam mixing technique of Dunham and Huntington (1970), for example, would allow the complete isolation of all the elastic constants for isotropic solids when the results are combined with the results of the present technique. At present, the beam mixing technique has not been adapted to cryogenic measurements.

2. Fused silica is one of several solids for which the thermal expansion coefficients change sign at certain temperatures. In the case of fused silica the change in sign is associated with transverse vibrational modes. Water also exhibits a change in sign of its thermal expansion coefficient at 4 °C. Since water is not known to support transverse acoustic waves, it would be interesting to investigate the ultrasonic nonlinearity characteristics of water using the present technique around that temperature. This would necessitate the development of a capacitive detector for liquids.

3. Fused silica is an anamolous material thermodynamically. There exist other isotropic materials which do not exhibit these anamolous properties and an investigation of their ultrasonic nonlinearity properties as a function of temperature may yield information which would help to characterize the difference between the materials.

4. Adapting the capacitive driver-capacitive receiver system to the cryogenic apparatus would eliminate any error introduced by the change of temperature in the transducer bonding material. It would also permit accurate measurements of ultrasonic velocity and attenuation in the samples as functions of temperature.

BIBLIOGRAPHY

Arnold, H., S. Hunklinger, S. Stein, K. Dransfeld, J. Non-Cryst. Solids 14, 192 (1974).

Bains, J. A., Jr., "Variations of Combinations of Third-Order Elastic Constants in Germanium between 3 and 300 °K," Ph.D. dissertation, University of Tennessee (1974).

_____ and M. A. Breazeale, J. Acoust. Soc. Am. 57, 745 (1975).

_____, Phys. Rev. B13, 3623 (1976).

Bajak, I. L., private communication, 1976.

Barker, L. M. and R. E. Hollenbach, J. Appl. Phys. 41, 4208 (1970).

Barron, T. H. K., Phil. Mag. 46, 720 (1955).

_____, Ann. Phys., N. Y. 1, 77 (1957).

Bateman, T., W. P. Mason, and H. J. McSkimin, J. Appl. Phys. 32, 928 (1961).

Benson, G. C. and O. Kiyohara, J. Acoust. Soc. Am. 55, 184 (1974).

Birch, F., Phys. Rev. 71, 809 (1947).

Blackman, M., Phil. Mag. 3, 831 (1958).

Breazeale, M. A. and J. Ford, J. Appl. Phys. 36, 3486 (1965).

Breazeale, M. A. and D. O. Thompson, Appl. Phys. Letters 3, 77 (1963).

Brugger, K., Phys. Rev. 133, A 1611 (1964).

_____ and T. C. Fritz, Phys. Rev. 157, 524 (1967).

Cantrell, J. H., Jr. and M. A. Breazeale, Proceedings, IEEE Ultrasonics Symposium, 537 (1974).

_____, to be published in J. Acoust. Soc. Am., February, 1977.

Clark, A. E. and R. E. Strakna, Physics Chem. of Glasses 3, 121 (1962).

Coldwell-Horsfall, R. A., Phys. Rev. 129, 22 (1963).

Collins, J. G., Phil. Mag. 8, 323 (1963).

Dunham, R. W. and H. B. Huntington, Phys. Rev. B2, 1098 (1970).

Fizeau, A. H. L., Pogg. Ann. Phys. 119, 87 (1863).

Flubacher, P., A. J. Leadbetter, J. A. Morrison, and B. P. Stoicheff, J. Phys. Chem. Solids 12, 53 (1959).

Fraser, D. B., J. Appl. Phys. 39, 5868 (1968).

W. B. Gauster, "Ultrasonic Measurements of the Nonlinearity Parameters of Copper Single Crystals," Ph.D. dissertation, University of Tennessee (ORNL-TM-1573, 1966).

_____ and M. A. Breazeale, Rev. Sci. Inst. 37, 1544 (1966).

_____, Phys. Rev. 168, 655 (1968).

Gedroits, A. A. and V. A. Krasilnikov, Sov. Phys. JETP 16, 1122 (1963).

Gerlich, D., Phys. Rev. B11, 1365 (1975).

Ghate, P. B., Phys. Rev. 139, A 1666 (1965).

Goldstein, H., Classical Mechanics. Addison-Wesley Publishing Company, Inc., Reading, Mass., 1965.

Graham, R. A., J. Acoust. Soc. Am. 51, 1576 (1972).

Green, Robert E., Jr., Ultrasonic Investigation of Mechanical Properties. Academic Press, New York, 1973.

Grüneisen, E., Handbuch der Physik 10, 1 (1926).

Hetherington, G. and K. H. Jack, Physics Chem. of Glasses 3, 129 (1962).

Hill, T. L., An Introduction to Statistical Thermodynamics. Addison-Wesley Publishing Company, Reading, Mass., 1962.

Hughes, D. S. and J. L. Kelley, Phys. Rev. 92, 1145 (1953).

Jones, G. L. and D. R. Kobett, J. Acoust. Soc. Am. 35, 5 (1963).

Klein, M. J. and R. D. Mountain, J. Phys. Chem. Solids 23, 425 (1962).

Leadbetter, A. J. and J. A. Morrison, Physics Chem. of Glasses 4, 188 (1963).

Legros, D., J. Lewiner, and P. Biquard, J. Acoust. Soc. Am. 52, 196 (1972).

Liebfried, G. and W. Ludwig, in F. Seitz and D. Turnbull, eds., Solid State Physics, Vol. 12. Academic Press, New York, 1961.

Mackey, J. E. and R. T. Arnold, J. Appl. Phys. 40, 4806 (1969).

May, J. E., Jr., IRE Nat. Conv. Record 6, Pt. 2, 134 (1958).

McCammon, R. D. and G. K. White, Phys. Rev. Letters 10, 234 (1963).

McSkimin, H. J., J. Acoust. Soc. Am. 33, 12 (1961).

_____ and P. Andreatch, J. Acoust. Soc. Am. 34, 609 (1962).

Meeks, E. L. and R. T. Arnold, Phys. Rev. B1, 982 (1972).

Papadakis, E. P., J. Acoust. Soc. Am. 42, 1045 (1967).

_____, J. Acoust. Soc. Am. 52, 843 (1972).

_____, J. Acoust. Soc. Am. 52, 847 (1972).

Peters, R. D., "Ultrasonic Measurement of the Temperature Dependence of Copper Nonlinearity Parameters," Ph.D. dissertation, University of Tennessee (ORNL-TM-2286, 1969).

_____, M. A. Breazeale, and V. K. Paré, Rev. Sci. Inst. 39, 1505 (1968).

_____, Phys. Rev. B1, 3245 (1970).

Primak, W., The Compacted States of Vitreous Silica. Gordon and Breach Science Publishers, New York, 1975.

Rollins, F. R., Jr., Appl. Phys. Letters 2, 147 (1963).

_____, L. H. Taylor, and P. H. Todd, Jr., Phys. Rev. 136, A 597 (1964).

Schuele, D. E. and C. S. Smith, J. Phys. Chem. Solids 25, 801 (1964).

Seki, H., A. Granato, and R. Truell, J. Acoust. Soc. Am. 28, 230 (1956).

Sheard, F. W., Phil. Mag. 3, 1381 (1958).

Simon, I., J. Amer. Ceram. Soc. 41, 116 (1958).

Slater, J. C., Introduction to Chemical Physics. McGraw-Hill Book Company, Inc., New York, 1939.

Taylor, R. H. and F. R. Rollins, Jr., Phys. Rev. 136, A 591 (1964).

Thurston, R. N., Physical Acoustics, Vol. 1A, Edited by W. P. Mason. Academic Press, New York, 1964.

_____ and K. Brugger, Phys. Rev. 133, A 1604 (1964).

Thurston, R. N. and M. J. Shapiro, J. Acoust. Soc. Am. 41, 1112 (1967).

Toupin, R. A. and B. Bernstein, J. Acoust. Soc. Am. 33, 216 (1961).

Voigt, W., Lehrbuch der Kristallphysik. Teubner, Leipzig und Berlin, 1928.

Warren, B. E., J. Appl. Phys. 8, 645 (1937).

White, G. K., Cryogenics , 2 (1964).

_____ and J. A. Birch, Physics Chem. of Glasses 6, 85 (1965).

Williams, J. and J. Lamb, J. Acoust. Soc. Am. 30, 308 (1958).

Yost, W. T., "An Ultrasonic Investigation of the Magnitude and Temperature Dependence of the Nonlinearity Parameters of Germanium and Fused Silica," Ph.D. dissertation, University of Tennessee, 1972.

_____ and M. A. Breazeale, J. Appl. Phys. 44, 1909 (1973).

_____, Phys. Rev. 139, 510 (1974).

Zachariesen, W. H., J. Amer. Chem. Soc. 54, 3841 (1932).

Zarembowitch, A., private communication, 1976.

APPENDIX

APPENDIX

THE EFFECT OF DIFFRACTION ON THE GATED DOUBLE-PULSE SUPERPOSITION METHOD OF ULTRASONIC VELOCITY MEASUREMENTS

The contributions of diffraction effects to accurate measurements of velocity and attenuation of ultrasonic waves is well known (Seki, Granato, and Truell, 1956; Papadakis, 1972). Correction formulas (Papadakis, 1967, 1972) for these diffraction effects have been derived for the ultrasonic pulse time-of-flight measurement techniques (Papadakis, 1967; McSkimin, 1961; May, 1958). The theory is now extended to provide corrections in velocity measurements utilizing the gated double pulse superposition method of Williams and Lamb (1958) (ultrasonic interferometer technique).

The problem is that of a circular piston transducer of radius a radiating an acoustic wave toward a coaxial circular receiver of the same dimension and at a distance z away. If it is assumed that the electrical response of the receiver is proportional to the average pressure over the receiver at a given time, the problem may be divided into two parts:

1. Find the acoustic pressure field at an arbitrary point $\vec{x}$ away from the transducer.
2. Average the generated acoustic pressure field over the surface of the receiving transducer.

If we let ϕ be the acoustic velocity potential, the acoustic pressure field may be found from the solution of the wave equation,

$$\nabla^2\phi = \frac{1}{c^2}\frac{\partial^2\phi}{\partial t^2}\,, \tag{A.1}$$

which satisfies the boundary condition,

$$\frac{\partial\phi}{\partial n} = u_0 \text{ (constant)}\,, \tag{A.2}$$

on the surface of the transmitting transducer. c is the sound velocity in Eq. (A.1), u_0 is the particle velocity, and $\frac{\partial}{\partial n}$ indicates normal derivation in Eq. (A.2).

The acoustic pressure is obtained from

$$p = \rho_0 \frac{\partial\phi}{\partial t} \tag{A.3}$$

where ρ_0 is the mean density of the sound propagation medium. The solution to Eq. (A.1) may be written as

$$\phi(\vec{x}) = -\frac{u_0}{2\pi}\int_{\sigma_1}\frac{e^{i(\omega t-\vec{k}\cdot\vec{r})}}{r}\,d\sigma_1 \tag{A.4}$$

where $\vec{r}$ is the distance from the surface element $d\sigma_1$ of the transmitting transducer to the field point $\vec{x}$, $\vec{k}$ is the wave number, ω is the angular frequency of the wave, and the integral is performed over the surface of the transmitting transducer. Substituting Eq. (A.4) into Eq. (A.3) gives

$$p(\vec{x}) = \frac{\omega\rho_0 u_0}{2\pi}\int_{\sigma_1}\frac{\sin(\omega t-\vec{k}\cdot\vec{r})}{r}\,d\sigma_1 - i\,\frac{\omega\rho_0 u_0}{2\pi}\int_{\sigma_1}\frac{\cos(\omega t-\vec{k}\cdot\vec{r})}{r}\,d\sigma_1\,. \tag{A.5}$$

The acoustic field pressure is the real part of $p(\vec{x})$.

Following Seki, Granato, and Truell (1956) one may evaluate the real part of Eq. (A.5)(in cylindrical polar coordinates) as

$$p(u,z,t) = X(u,z)\cos(\omega t-kz) + Y(u,z)\sin(\omega t-kz) \tag{A.6}$$

where z is the direction perpendicular to the surface of the transmitting transducer, u is measured perpendicular to the z direction at some distance z from the transducer, and

$$X(y,z) = V_0 \cos\frac{k(x^2+a^2)}{2z} + V_1 \sin\frac{k(x^2+a^2)}{2z} - 1 \tag{A.7}$$

$$Y(u,z) = V_0 \sin\frac{k(x^2+a^2)}{2z} - V_1 \cos\frac{k(x^2+a^2)}{2z} \tag{A.8}$$

and

$$V_0 = \sum_{n=0}^{\infty} (-1)^n \left(\frac{u}{a}\right)^{-2n} J_{2n}\left(\frac{kau}{z}\right) \tag{A.9}$$

$$V_1 = \sum_{n=0}^{\infty} (-1)^n \left(\frac{u}{a}\right)^{-2n-1} J_{2n+1}\left(\frac{kau}{z}\right) . \tag{A.10}$$

This completes part (1) of the problem.

The average of the generated acoustic pressure field over the surface of the receiving transducer may be written as

$$\langle p(z)\rangle = \frac{1}{\sigma_2}\int_{\sigma_2} p\,d\sigma_2 \tag{A.11}$$

where σ_2 is the surface area of the receiving transducer. Substituting Eq. (A.6) into (A.11) gives

$$\langle p(z)\rangle = \frac{1}{\sigma_2}\left[\cos(\omega t-kz)\int_{\sigma_2} X\, d\sigma_2 - \sin(\omega t-kz)\int_{\sigma_2} Y\, d\sigma_2\right] . \qquad (A.12)$$

We may rewrite (A.12) in the form

$$\langle p(z)\rangle = \langle p\rangle_{max}\cos[\omega t-kz-\phi(z)] \qquad (A.13)$$

where

$$\langle p\rangle_{max} = \frac{1}{\sigma_2}\left[\left(\int_{\sigma_2} X\, d\sigma_2\right)^2 + \left(\int_{\sigma_2} Y\, d\sigma_2\right)^2\right]^{1/2} \qquad (A.14)$$

and

$$\phi(z) = \tan^{-1}\left[\frac{\int_{\sigma_2} Y\, d\sigma_2}{\int_{\sigma_2} X\, d\sigma_2}\right] . \qquad (A.15)$$

Benson and Kiyohara (1974) have evaluated numerically Eqs. (A.13) and (A.15) as a function of the dimensionless parameter,

$$S = \frac{z\lambda}{a^2} , \qquad (A.16)$$

where λ is the ultrasonic wavelength.

For the ultrasonic interferometer technique we must consider two pulse-echo trains, the second pulse-echo train being delayed with respect to the first such that superposition of the two trains is achieved. If attenuation of the echo signals is neglected, the total average pressure at the receiving transducer due to a given pair of superimposed echoes may be written as

$$\langle p\rangle_T = \langle p\rangle_{max} \{\cos[\omega t - k(m+1)\ell - \phi(S_m)] + \cos[\omega t - k(2n+1)\ell - \phi(S_n)]\} \tag{A.17}$$

where ℓ is the distance between the transmitting and receiving transducers (sample length), m and n are integers representing the number of round trips through the sample of the initial and delayed pulses (i.e., the echo numbers), and

$$S_m = \frac{z_m \lambda}{a^2} = \frac{(2m+1)\ell\lambda}{a^2} . \tag{A.18}$$

Thus, we may write

$$\langle p\rangle_T = 2\langle p\rangle_{max} \cos\left\{\omega t - k\ell(m+n+1) - \frac{\phi(S_m)+\phi(S_n)}{2}\right\}$$

$$X \cos\left\{k\ell(m-n) + \frac{\phi(S_m)-\phi(S_n)}{2}\right\}. \tag{A.19}$$

Nulls in $\langle p\rangle_T$ occur at

$$k\ell(m-n) + \frac{\phi(S_m)-\phi(S_n)}{2} = \left(\frac{2q+1}{2}\right)\pi \tag{A.20}$$

where q = integer. If we consider two nulls of Eq. (A.19) at q_1 and q_2 and write

$$k = \frac{2\pi f}{v} \tag{A.21}$$

where f is the ultrasonic frequency and v is the ultrasonic velocity, then we may write from Eq. (A.20)

$$v = 2p\ell \frac{\Delta f}{\Delta q} \left(1 - \frac{1}{2\pi} \frac{\Delta\phi}{\Delta q}\right)^{-1} \qquad (A.22)$$

where $p = m-n$ and $\Delta f = f_2-f_1$ is the change in ultrasonic frequency corresponding to $\Delta q = q_2-q_1$ minima (nulls) of the superimposed pulse-echo trains. The quantity used in the calculations is written in the form

$$\Delta\phi = \frac{1}{2} \{\phi(S_{n1}) - \phi(S_{n2}) + \phi(S_{m2}) - \phi(S_{m1})\} \qquad (A.23)$$

where

$$\phi(S_{ij} = \phi\left(\frac{(2i+1)\ell v}{a^2 f_j}\right) \qquad (A.24)$$

and

$i = m, n$

$j = 1, 2.$

Equation (A.22) is the equation for calculating the ultrasonic phase velocity including the diffraction correction factor $\left(1 - \frac{1}{2\pi} \frac{\Delta\phi}{\Delta q}\right)^{-1}$. Note that for $\Delta\phi=0$ (i.e., no diffraction effects), the equation reduces to Eq. IV.21, page 56.